

AN ABSTRACT OF THE THESIS OF

Nevenka Obuskovic for the degree of Master of Science
in Chemical Engineering presented on April 19, 1985.

Title: Heat Transfer Between Moving Beds of Solids and a Transverse
Finned Tube

Abstract approved:

Redacted for Privacy

Dr. James G. Knudsen

The objective of this research is to measure the rate of heat transfer between a transverse finned tube and a moving bed of particles. This was done under steady-state conditions.

An empirical equation was developed employing dimensional analysis and nonlinear regression of the experimental data:

$$Nu_d = 2.37 Pe_d^{0.25} \left(\frac{k_e}{k_g}\right)^{0.3} \left(\frac{d_p}{L}\right)^{0.33}$$

This equation predicts the heat transfer coefficients for plain and finned tubes within ± 20 percent, but is restricted to the tubes with fin heights equal to or smaller than the one used for this research.

It was observed that the heat transfer coefficient is higher for the particles with smaller diameters as compared to the larger diameter particles of the same substance. Also that the heat transfer coefficient is dependent on the velocity of the particle flow over the heated surface.

Heat Transfer Between Moving Beds of Solids and
a Transverse Finned Tube

by

Nevenka S. Obuskovic

A THESIS

submitted to

Oregon State University

in partial fulfillment of
the requirements for the
degree of

Master of Science

Completed April 19, 1985

Commencement June 1985

APPROVED:

Redacted for Privacy

Professor of Chemical Engineering in charge of major

Redacted for Privacy

Chairman of Chemical Engineering Department

Redacted for Privacy

Dean of Graduate School

Date thesis is presented April 19, 1985

Typed by Meredith Turton for Nevenka Obuskovic

ACKNOWLEDGEMENTS

The author would like to express her deep gratitude to Dr. Octave Levenspiel for his suggestions, assistance and continued active interest in this work.

I would also like to express my most sincere thanks and appreciation to Dr. James G. Knudsen for his kind advice, assistance and encouragement during the course of this research; also for reading and correcting the manuscript and the final draft.

Grateful acknowledgments are also extended to my dear professors and chairman, Dr. Charles Wicks and Dr. Robert Mrazek for enormous understanding and support in the completion of this thesis.

I wish to express gratitude to Dr. Manuk Colakyan for his assistance and suggestions, which he gave unselfishly. I would also like to express my gratitude to Dick Turton and to my countryman, Dr. Aleksandar Dudukovic who cooperated successfully with me for the last few months of this thesis work.

My thanks also go to Nick Wannemacher for his invaluable help in experimental research whenever necessary.

Finally, I wish to express special thanks to my professor Dr. Goran Jovanovic (University of Belgrade) for his suggestions and help in my coming to Oregon State University.

I also want to thank the rest of the faculty members for their help and encouragement during the course of this research.

Last, but not least, the author would like to extend her thanks towards Mrs. Meredith Turton for typing the final draft.

NOMENCLATURE

<u>Symbol</u>	<u>Description</u>	<u>Units</u>
A	- cross sectional area of the bed	m ²
A _B	- area of the tube without fins	m ²
A _T	- heat transfer area (surface area of the finned tube)	m ²
C _{ps}	- heat capacity of solids	J/kgK
d _f	- fin diameter	m
d _p , \bar{d}_p	- particle diameter or surface mean particle diameter	m
d _{pi}	- diameter of particles of size "i"	m
e	- fin height	m
h	- heat transfer coefficient between finned tube and granular media	W/m ² K
f _D (f _w)	- friction coefficient between a tube and dry (wet) solids	
h _i	- local heat transfer coefficient	
k _g	- thermal conductivity of gas	W/mK
k _e	- effective thermal conductivity of solids-gas emulsion	W/mK
k _s	- thermal conductivity of solids	W/mK
L	- heat length across the flow path of solids (characteristic length)	m
L _B	- half of the parameter of the tube	m
L _F	- half of the parameter of the finned tube	m
L _R	- length of the finned tube	m
N _F	- number of fins	

<u>Symbol</u>	<u>Description</u>	<u>Units</u>
$Nu_d = \frac{hd_p}{k_g}$	- Nusselt number based on particle diameter	
P	- power	W
$Pe = \frac{C_{ps} d_p \rho_b U_s}{k_g}$	- Peclet number based on particle diameter (d_p)	
r	- outside radius of the tube (no fins)	m
R	- radius of the fin (from the center of tube)	m
R_c	- contact resistance (due to gas film)	m^2K/W
R_e	- average emulsion resistance	m^2K/W
R_{ex}	- local emulsion resistance at distance "X" from the heater; in the flow direction	m^2K/W
R_{eL}	- local emulsion resistance at distance L from the edge of the heater; in the flow direction	m^2K/W
R_Ω	- resistance of the cartridge heater	Ω
s	- fin spacing	m
$T = T(X,Y)$	- temperature at "X" and "Y" points	K
T_g	- temperature of the gas	K
T_s	- bulk temperature of the solids	K
T_R	- steady-state average surface temperature of the rod	K
t	- time	s
U_s	- linear solids velocity	m/s
V	- potential difference	volts
W_s	- mass flow rate of solids	kg/s
X	- distance in the flow direction	m

<u>Symbol</u>	<u>Description</u>	<u>Units</u>
X_i	- mass fraction of particles of size " i "	.
Y	- distance from the heater surface normal to the flow	m

GREEK SYMBOLS

<u>Symbol</u>	<u>Description</u>	<u>Units</u>
α_e	- effective thermal diffusivity (emulsion)	m^2/s
α_s	- effective thermal diffusivity (solids)	m^2/s
δ	- average gas thickness	m
ϵ	- porosity of the packed bed	
ρ_b, ρ_e	- bulk density of the solids	kg/m^3
ρ_s	- density of solid materials	kg/m^3
τ_D, τ_W	- effective shear stress for dry and wet solids, respectively	N/m^2

TABLE OF CONTENTS

<u>Chapter</u>	<u>Page</u>
I. INTRODUCTION	1
II. PREVIOUS WORK	2
III. EXPERIMENTAL EQUIPMENT	5
A. Heated Finned Tube	5
B. The Moving Bed	7
C. Materials	7
IV. EXPERIMENTAL PROCEDURE	17
A. Measurement of the Heat Transfer	17
B. Velocity Measurements	17
V. EXPERIMENTAL RESULTS	21
A. Calculation of Heat Transfer Coefficients	21
B. Heat Transfer Results - Graphical Presentation	22
VI. CORRELATION EQUATION	29
VII. DISCUSSION OF COLAKYAN'S MODEL	35
A. Colakyan's Work	35
B. Analysis of Colakyan's Model	45
VIII. CONCLUDING STATEMENTS	50
BIBLIOGRAPHY	52
APPENDIX	55

LIST OF FIGURES

<u>Figure</u>		<u>Page</u>
(III.1)	The instrumented and heated finned tube.	6
(III.2)	General layout of moving bed apparatus (reproduced from Colakyan (9)).	8
(III.3)	A moving grate (reproduced from Colakyan (9)).	9
(III.4)	A pneumatic solids transport system (reproduced from Colakyan (9)).	10
(IV.1)	The dependence of linear velocity (M_s) to mass flow rate (W_s) (measured in the 14 x 16 cm test section), for 0.85 mm and 1.6 mm polyethylene and 0.27 mm and 1.01 mm copper particles: ----- calculated, _____ measured.	19
(IV.2)	The dependence of linear solids velocity (s) to mass flow rate (W_s) (measured in the 14 x 16 cm test section), for 0.27 mm, 0.8 mm, and 1.1 mm silica sand particles: ----- calculated, _____ measured.	20
(V.1)	Comparison between heat transfer coefficients as a function of the linear velocity of the solids for polyethylene particles of 0.85 mm and 1.6 mm in diameter.	24
(V.2)	Comparison between the heat transfer coefficients for a finned and plain tube for polyethylene particles of 1.6 mm in diameter.	25
(V.3)	Comparison between the heat transfer coefficients for a finned and plain tube for polyethylene particles of 0.85 mm in diameter.	26
(V.4)	Comparison between heat transfer coefficients for polyethylene and silica sand with diameters 0.85 mm and 0.8 mm, respectively.	27

<u>Figure</u>		<u>Page</u>
(V.5)	Comparison between heat transfer coefficients for copper and silica sand with diameters 0.85 mm and 0.8 mm, respectively.	28
(VI.1)	Predicted (from Equation VI.8) and observed Nusselt number for all particles and sizes used for the experiment.	32
(VI.2)	Predicted (from equation VI.8) and observed Nusselt numbers for all particles and sizes (data for heat transfer coefficients taken from Colakyan (9)).	33
(VI.3)	Predicted (from equation VI.8) and observed Nusselt numbers from Colaykan's (9) and author's data for all particles and sizes.	34
(VII.1)	Comparison of the continuum model for planar and cylindrical geometrics with set of experimental data (reproduced from Colakyan (9)).	36
(VII.2)	Temperature profiles, in the semi-infinite plane above a constant temperature, heated flat plate, for a contact time of 3.5 s (reproduced from Colakyan (9)).	40
(VII.3)	A comparison of model predictions (two thermal resistances, R_e and R_c , in series with $R_c = 0.00168 \text{ m}^2\text{K/W}$) with experimental results, for 0.85 mm polyethylene particles (reproduced from Colakyan (9)).	43
(VII.4)	A comparison of model predictions (two thermal resistances, R_e and R_c , in series with $R_c = 0.0057 \text{ m}^2\text{K/W}$) with experimental results, for 1.6 mm polyethylene particles (reproduced from Colakyan (9)).	44

<u>Figure</u>		<u>Page</u>
(VII.5)	Predicted (from equation VI.8) and observed Nusselt numbers, for all particles and sizes (reproduced from Colakyan (9)).	46
(VII.6)	Contact resistance (R_c) vs. linear solids velocities for all particles and sizes.	48

LIST OF TABLES

<u>Table</u>		<u>Page</u>
(III.1)	Properties of Materials Used and Operating Conditions.	12
(III.2)	Solids Properties.	13
(III.3)	Size Distributions of Particles.	14
<u>Appendix</u>		
A.1	Table of Experimental Conditions and Heat Transfer Coefficients for Polyethelene Particles.	55
A.2	Table of Experimental Conditions and Heat Transfer Coefficients for Silica Sand Particles.	56
A.3	Table of Experimental Conditions and Heat Transfer Coefficient for Copper Particles.	58

HEAT TRANSFER BETWEEN MOVING BEDS OF SOLIDS AND A TRANSVERSE FINNED TUBE

I. INTRODUCTION

The study reported in this thesis is concerned with the rate of heat transfer between transverse finned tubes and a moving bed of solid particles.

One of the problems with which a chemical engineer is confronted is the prediction of process rates in all types of equipment in order to select the type which is the best to use.

In order to attain maximum rates of heat transfer attempts to increase the amount of heat transfer area in a given space have resulted in the development of a wide variety of extended surface tubes.

Recently Colakyan (9) investigated heat transfer from a plain tube to moving beds of solids. He showed that his experimental results corresponded well to a model in which the convective heat transfer coefficient depends on two resistances (R_e and R_c) in series.

The present study involves the forced convective heat transfer from a single finned tube immersed in a flowing granular material. The scope of the study is to provide some basic data for predicting heat transfer coefficients as a function of the moving bed parameters and the bed flow rate.

II. PREVIOUS WORK

A considerable amount of work has been done on the flow characteristics, as well as heat transfer behavior, of granular media in systems such as: fluidized and packed beds. However, the mechanism of convective heat transfer to/from surfaces immersed in flowing solids is not yet well understood. Related previous work is briefly reviewed in this chapter.

Mickley and Fairbanks (1) were among the first to obtain data for the instantaneous heat transfer coefficient in fluidized beds and developed the original version of the "packet" theory. The packet (the group of particles) was assumed to be in contact with the heated surface for a short time and then replaced by a new packet from the bulk of the bed. They considered the packet to be homogeneous with uniform thermal properties and they expressed the local instantaneous heat transfer coefficient as

$$h_i = \sqrt{\frac{k_e C_{ps} \rho_b}{\pi t}}$$

Harakas and Beatty (2) considered the heat transfer from a flat plate immersed in rotating beds of granular material. They varied particle size as well as interstitial gas, and found an increase in average heat transfer coefficient with decrease in the particle diameter. Fine grained materials were considered to be one-component continuum. However, greater discrepancies in the model predictions occurred as the particle size increased. This

result is expected since the thermal gradient which forms within the "packet" in a short residence time does not extend more than one or two particle diameters from the surface.

The convective heat transfer from a flat plate to various granular materials flowing parallel to the plate was investigated by Sullivan and Sabersky (3). To explain their observations they used a discrete particle model. In this model it was assumed that the conductance at the wall was the same as that existing between adjacent rows of particles and that the conductance was inversely proportional to the average thickness of the gas film between particles and the heated plate. The value of the wall resistance was found to be equivalent to an air film of 1/10 of a particle diameter.

Studying the mechanism of heat transfer between a fluidized bed and immersed surfaces Baskakov (4) introduced an additional contact resistance R_c , in series with the thermal resistance of the packets, R_e , as defined by Mickley and Fairbanks (1) contact resistance R_c is assumed to mean the additional thermal resistance of the layer next to the wall, which is due to increased porosity.

Denloye and Botterill (5) studied the heat transfer in flowing packed beds. They obtained data by varying the particle sizes of different materials, i.e., copper shot, sand, coal ash and soda glass and by using different interstitial gases. They concluded that the heat transfer coefficient increases with increasing gas thermal conductivity, decreasing particle size and particle residence time.

Spelt (6) investigated the heat transfer to a granular material flowing in an inclined chute. He found that the heat transfer coefficient increased to a maximum and then decreased as the velocity of the solids across the plate increased.

Russian researchers Donskov and Kurockin also experimented with flowing packed beds.

Donskov (7) investigated the heat transfer coefficient, by varying the tube diameter and pitch of the tubes in a tube bank. The results showed that the heat transfer coefficient increases with a decrease in the ratio between pitch and tube diameter. Kurockin (8) investigated the heat transfer coefficient between dry and wet material, and a single tube. He concluded that heat transfer was increased as the velocities of the granular material increased, and he correlated his results with the following equation:

$$Nu_D = 0.22 P_{eD} \left(\frac{D}{d_p} \right) \left(\frac{f_d}{f_w} \right) \left(\frac{\tau_D}{\tau_W} \right)^{0.33}$$

Colakyan's (9) work on heat transfer from a single tube to various granular materials flowing in a direction perpendicular to the cylinder axis most closely resembles the present investigation. The value of the contact resistance R_c first introduced by Baskakov (4) was determined empirically from the experimental data. The resistance was estimated to be

$$R_c = \frac{6.7 \times 10^{-5} d_p^2}{k_g}$$

III. EXPERIMENTAL EQUIPMENT

A. Heated Finned Tube

The main scope of this investigation is the determination of the heat transfer coefficient between extended surfaces (transverse finned tube) and free flowing granular material. Various granular material were allowed to flow past a 0.4572 m long, horizontal heated finned tube, for experimental determination of heat transfer coefficients.

The instrument, illustrated in Figure (III.1) consists of a solid copper crimped-finned tube 0.022 m O.D., 0.4572 m long with 54 transverse fins having a diameter $d_f = 0.0349$ m; fin height $e = 6.35 \times 10^{-3}$ m; fin spacing $s = 8.5 \times 10^{-3}$ m; and fin thickness = 2.8×10^{-4} m.

Heating was provided by a WATLOW, 5000 W (N18A15) heater cartridge inserted tightly into the finned tube. Ten, 36 gauge K type thermocouples were soldered to the fins. Six of these thermocouples were located in the middle of the rod placed at the top and the base of the fin at 0, 90, and 180 degrees from the top. Two thermocouples were attached 0.114 m from one end of the tube cemented to the top and the bottom of the fin. The remaining two were placed at the end of the rod in a similar fashion. The bulk temperature of the material was measured at a point 0.2 m above the heated surface. The temperature of the flowing material was essentially equal to the temperature prior to entering the bed. All the temperatures were recorded by two analog AD2036 thermocouple readers.

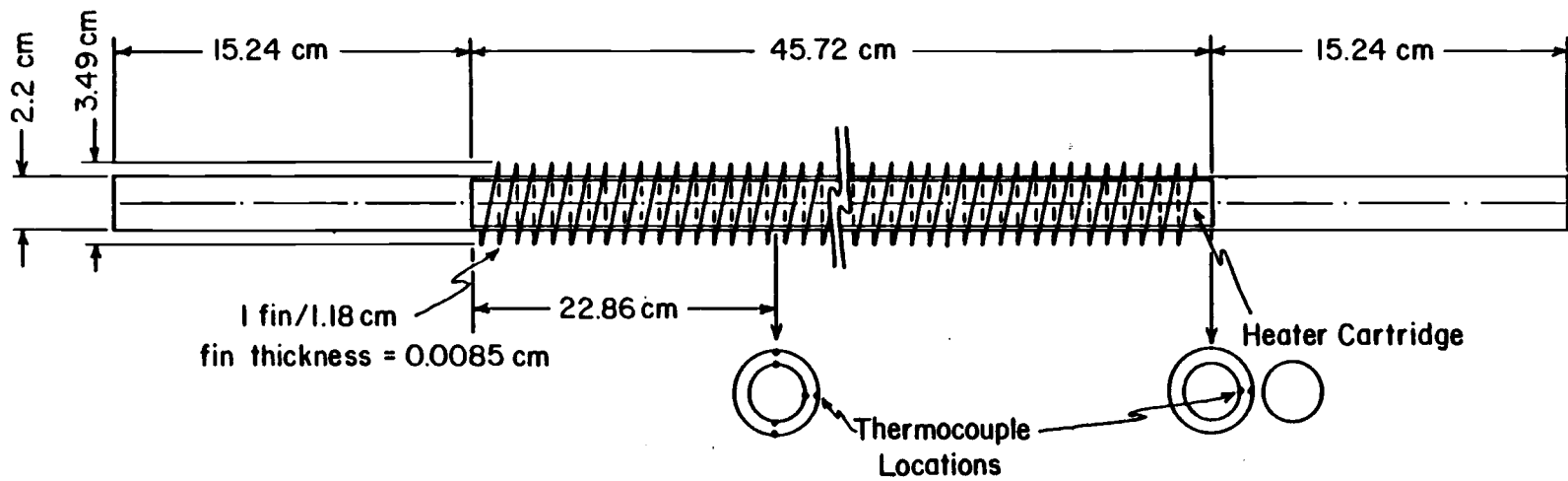


Figure (III.1) The Instrumented and Heated Finned Tube

B. The Moving Bed

The experiments were completed with the same moving bed as used by Colakyan (9) (Figure III.2). The unit was made of steel, 3 m in height and 30 x 46 cm in cross-section. Dimensions of the actual measuring section were 14 x 46 cm with the rod assembly placed in the center of the section.

Two plexiglass side windows permitted visual observation and the measurement of the velocity of the flowing solids adjacent to the wall. For this purpose a 30 cm long measuring tape was placed parallel to the flow direction outside the window. To provide a uniform flow of solids, a moving grate (Figure III.3) was installed at the base of the bed. Different velocities were obtained by varying the frequency and amplitude of the moving grate. Since the higher frequencies gave a smoother flow, the frequency was always set at a maximum of 340 RPM and only the amplitude was varied. The flow rate of the solids was independent of the material height in the bed.

A pneumatic transportation line (Figure III.4) was used to transfer the solids collected in the hopper under the grate to the top of the bed. A Sutorbilt blower provided the air for the transportation system at $1.33 \text{ m}^3/\text{min}$ and 185kPa.

C. Materials

In the present work only granular materials are considered. Porous materials in which a solid medium has a closed gaseous space

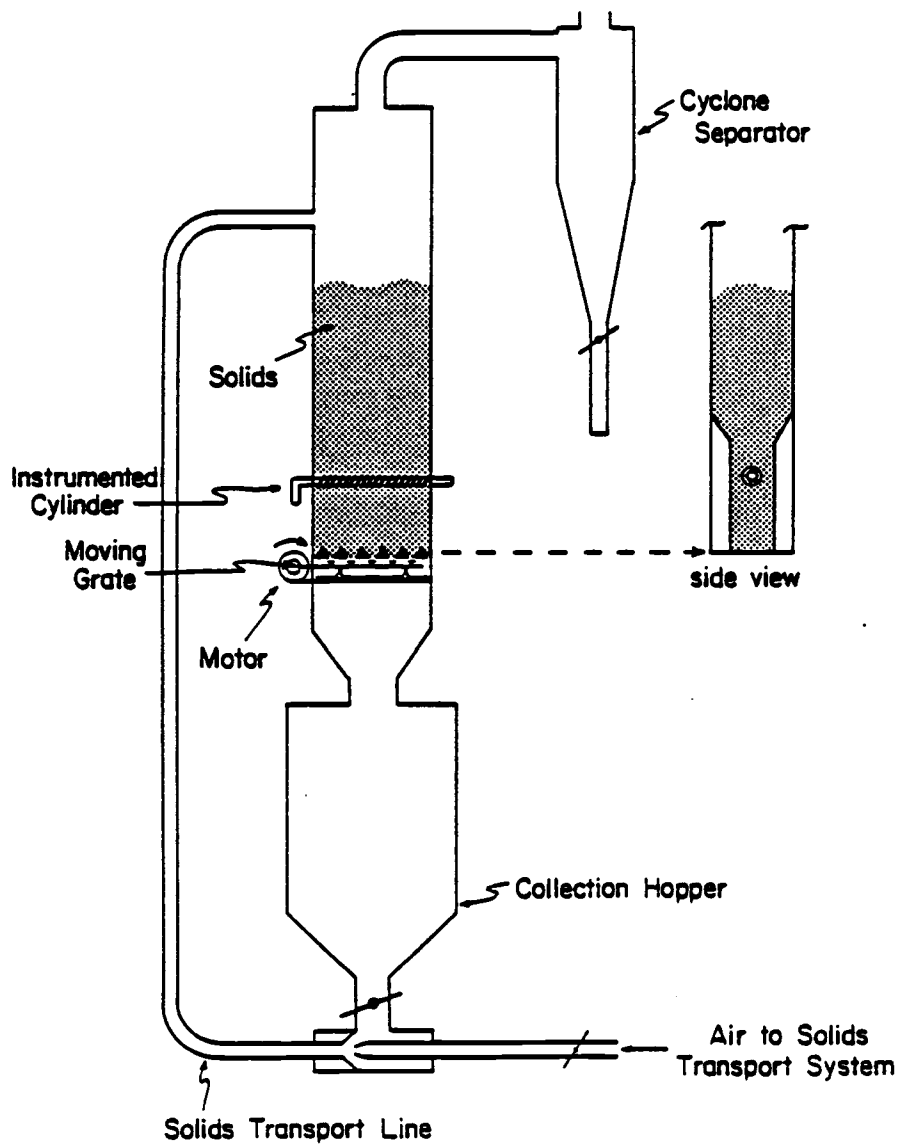
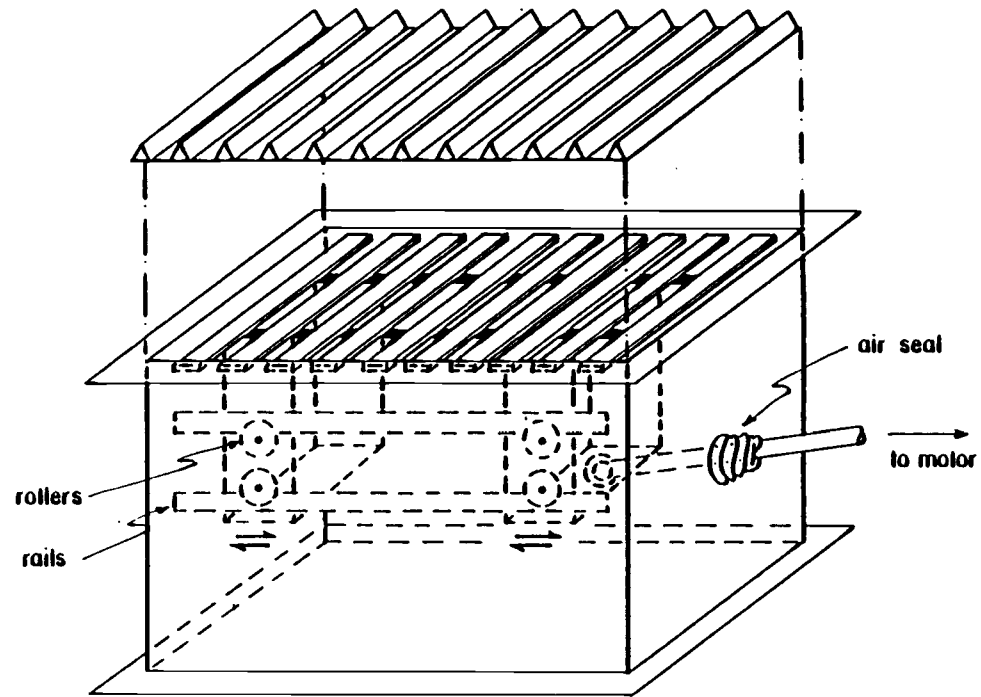


Figure (III.2). General Layout of Moving Bed Apparatus (reproduced from Colakyan (9))



Solids Flow Controller-Moving Grate

Figure (III.3). A Moving Grate (reproduced from Colakyan (9))

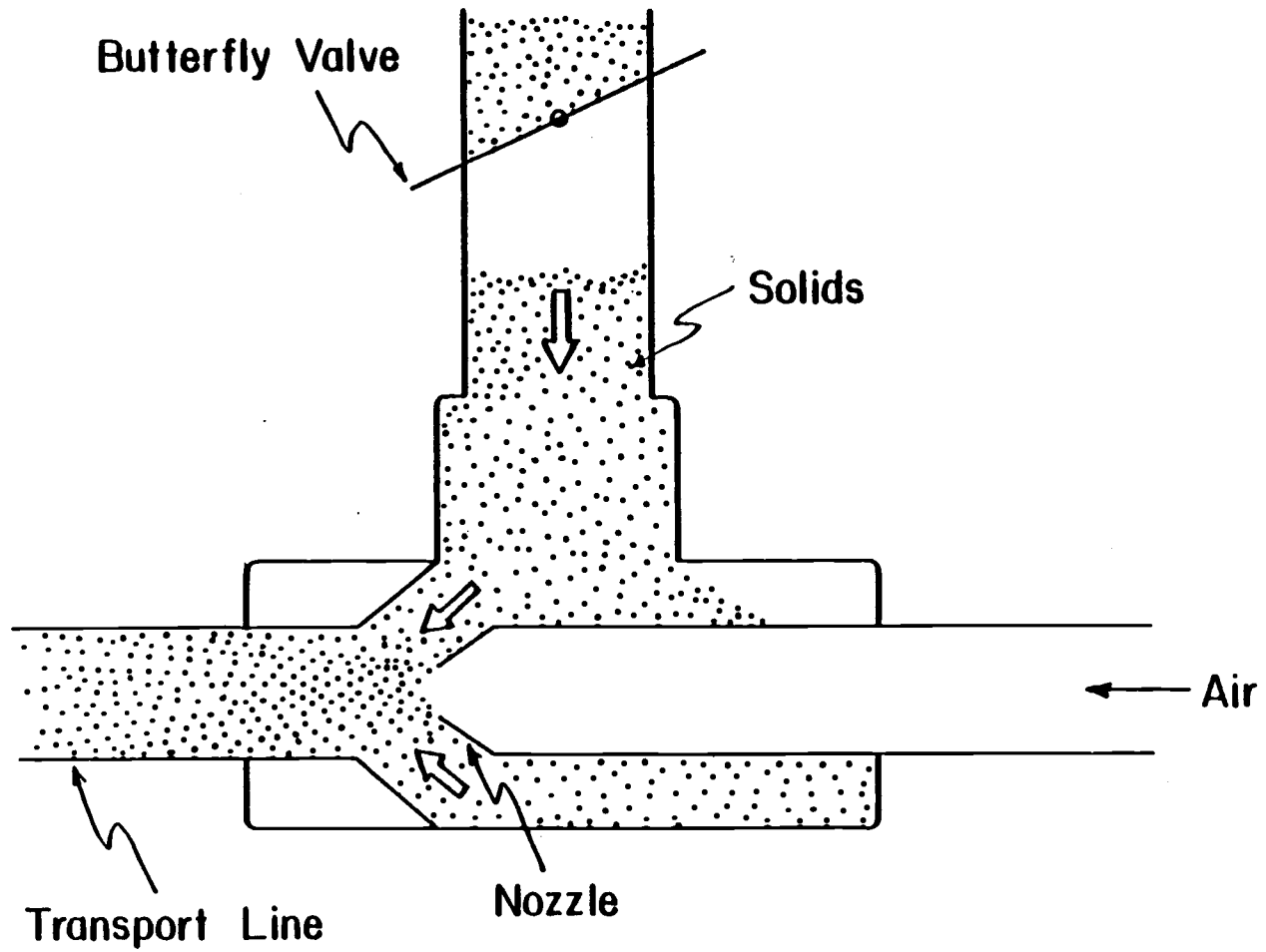


Figure (III.4). A Pneumatic Solids Transport System (reproduced from Colakyan (9))

were not considered. Three types of solids, polyethylene, sand and copper were used as the granular media. Properties of the materials used in the experiments as well as range of operating conditions are given in Table (III.1).

Table (III.2) lists all the properties of three different solids used in the experiments.

Materials available for the experiments had a wide size distribution and their mean diameter was calculated according to the following formula

$$d_p = \frac{1}{\sum \frac{x_i}{d_{p_i}}}$$

where x_i = mass fraction of particles of size "i"

d_{p_i} = diameter of particles of size "i."

Table (III.3) gives the size distribution of the particles used in the experiment.

Table (III.1). Properties of Materials Used and Operating Conditions

<u>Material</u>	<u>Range of Operating Conditions</u>
Particle Diameter, d_p	= 0.11 - 1.6 mm
Solids Density, ρ_s	= 920 - 8950 kg/m ³
Bulk Density, ρ_b	= 345 - 5360 kg/m ³
Solids Thermal Conductivity, k_s	= 0.33 - 384 w/mk
Solids Heat Capacity, C_{ps}	= 380 - 2300 w/mk J/kgK
Linear Solids Velocity, U_s	= 0.002 - 0.025 m/s
Mass Flow Rate, W_s	= 0.04 - 6.1

Table (III.2). Solids Properties

Material	d_p (mm)	k_s (W/m·K)	ρ_s (kg/m ³)	C_{ps} (J/kg·K)	ϵ	ρ_b (kg/m ³)	k_e (W/m·K)	$\alpha_e \times 10^8$ (m ² /s)	$\alpha_s \times 10^7$ (m ² /s)
Polyethylene	0.85	0.329	920	2300	0.6	365	0.07	8.34	1.555
Polyethylene	1.6	0.329	920	2300	0.625	345	0.063	7.94	1.555
Sand	0.11	0.8	2700	780	0.53	1280	0.140	14.02	3.799
Sand	0.8	0.8	2700	780	0.48	1410	0.171	15.5	3.799
Sand	1.2	0.8	2700	780	0.47	1440	0.182	16.2	3.799
Copper	0.21	384	8950	383	0.4	5360	0.46	22.4	1120
Copper	0.85	384	8950	383	0.42	5200	0.41	20.5	1120

Values for effective properties are calculated for stagnant gas using Equation (VII.4).

Table (III.3). Size Distributions of Particles

Polyethylene

$\bar{d}_p \sim 1.6 \text{ mm}$		$\bar{d}_p \sim 0.85 \text{ mm}$	
<u>Tyler Mesh</u>	<u>% Weight</u>	<u>Tyler Mesh</u>	<u>% Weight</u>
-6 + 9	43.65	-20 + 24	44.58
-9 + 14	38.4	-24 + 28	21.07
-14 + 20	12.61	-28 + 35	16.85
-20 + 24	2.33	-35	17.5
-24 + 28	1.45		
-28	1.56		

Silica Sand

$\bar{d}_p \sim 0.11 \text{ mm}$			
<u>Tyler Mesh</u>	<u>% Weight</u>	<u>Tyler Mesh</u>	<u>% Weight</u>
-42 + 60	2.18	-20 + 24	35
-60 + 80	5.5	-24 + 28	21.37
-80 + 100	9.57	-28 + 35	21.16
-100 + 115	17.83	-35 + 48	15.21
-115 + 150	19.2	-48	7.26
-150 + 170	16.37	<u>Tyler Mesh</u>	<u>% Weight</u>
-170 + 200	13.4	-10 + 14	67.84
-200 + 250	6.77	-14 + 20	31.35
-250 + 270	5.25	-20 + 24	0.693
-270 + 325	2.5	-24	0.218
-325	1.43		

Table (III.3) continued

Silica Sand

$\bar{d}_p \sim 0.11 \text{ mm}$		$\bar{d}_p \sim 0.8 \text{ mm}$	
<u>Tyler Mesh</u>	<u>% Weight</u>	<u>Tyler Mesh</u>	<u>% Weight</u>
-42 + 60	2.18	-20 + 24	35
-60 + 80	5.5	-24 + 28	21.37
-80 + 100	9.57	-28 + 35	21.16
-100 + 115	17.83	-35 + 48	15.21
-115 + 150	19.2	-48	7.26
-150 + 170	16.37	$\bar{d}_p \sim 1.2 \text{ mm}$	
-170 + 200	13.4	<u>Tyler Mesh</u>	<u>% Weight</u>
-200 + 250	6.77	-10 + 14	67.84
-250 + 270	5.25	-14 + 20	31.25
-270 + 325	2.5	-20 + 24	0.693
-325	1.43	-24	0.218

Table (III.3) continued

Copper

$\bar{d}_p \sim 0.214 \text{ mm}$		$\bar{d}_p \sim 0.85 \text{ mm}$	
<u>Tyler Mesh</u>	<u>% Weight</u>	<u>Tyler Mesh</u>	<u>% Weight</u>
-20 + 24	0.3	-14 + 20	33.94
-24 + 28	0.78	-20 + 24	62.2
-28 + 32	5.24	-24 + 28	3.05
-32 + 48	43.3	-28 + 32	0.39
-48 + 60	1.75	-32 + 35	0.19
-60 + 80	17.52	-35 + 40	0.18
-80 + 100	11.70	-40	0.05
-100 + 115	3.39		
-115 + 150	3.78		
-150 + 170	4.98		
-170	7.26		

IV. EXPERIMENTAL PROCEDURE

In the present work heat was transferred by convection between a solid surface (finned tube) and the solid particles moving relative to the surface. The adjacent particles were in physical contact and the interstitial fluid (air) was carried along with the particles. Experiments were performed at atmospheric pressure.

A. Measurements of the Heat Transfer

The heat transfer coefficients were measured under steady-state conditions. Electric power to the heater was supplied by a rheostat and was regulated by adjusting the voltage across it. First, the grate was set at a certain speed allowing the granular media to flow over the instrumented cylinder and then the power was turned on. The temperature change was followed using a calibration chart for the thermocouples. For more details, the reader is referred to Colakyan (9). Steady-state was reached when the temperature variation with time was negligible. The ends of the rod were well insulated and the temperatures along the rod varied within a few degrees Celcius.

B. Velocity Measurements

The velocity was measured in two different ways as was done by Colakyan (9):

1. The amount of solids from the bed outlet in a given time was collected and weighted. Knowing the properties of the

material and the cross sectional area available for flow, velocity was estimated using the following relationship:

$$U_s = \frac{\text{mass flow rate}}{(\text{bulk density})(\text{flow area})} \quad (\text{IV.1.1})$$

2. This method assumes that solids are flowing in plug flow. The velocities were estimated by visual observation of the particles near the transparent wall; by measuring the time taken for the particles to move a given distance.

Figures (IV.1 and 2) reproduced from Colakyan (9), show a good agreement between velocity measured by this method and that determined by weighing solids discharged over a given time.

For data analysis, velocities measured by method (1) were used.

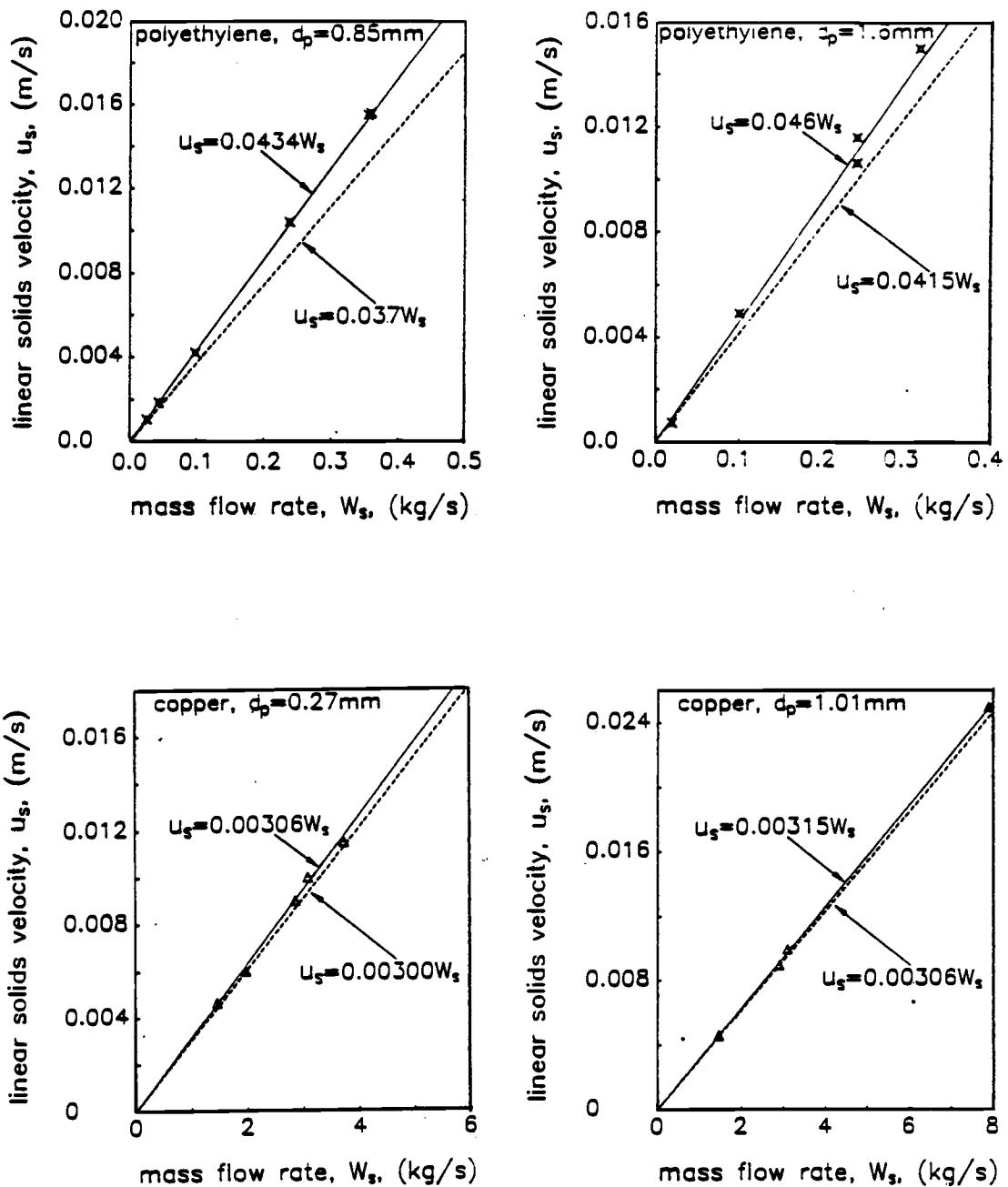


Figure (IV.1). The dependence of linear velocity (U_s) to mass flow rate (W_s), (measured in the 14×16 cm test section), for 0.85 mm and 1.6 mm polyethylene and 0.27 mm and 1.01 mm copper particles; ----- calculated, _____ measured (reproduced from Colakyan (9)).

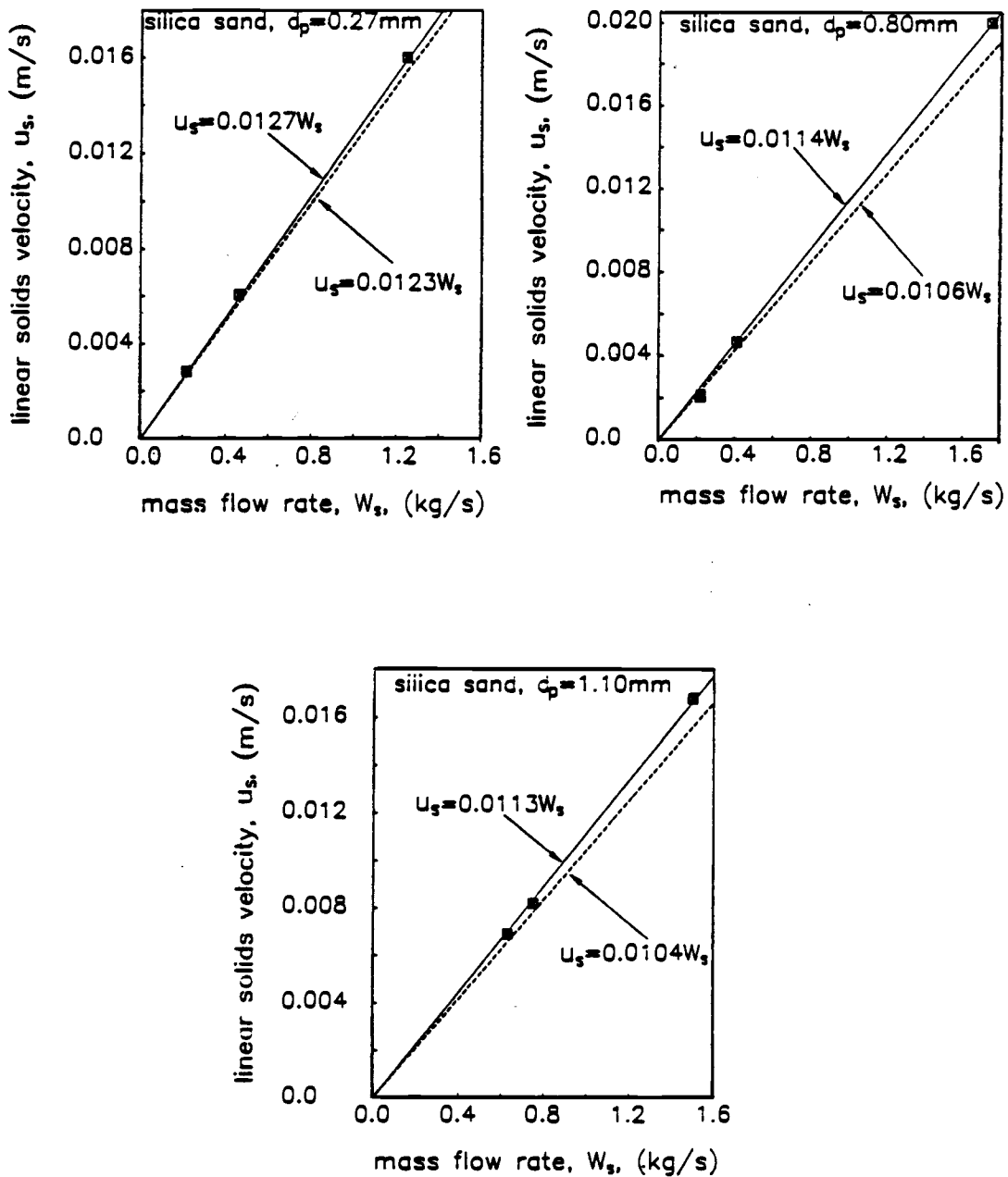


Figure (IV.2). The dependence of linear velocity (U_s) to mass flow rate W_s (measured in the 14 x 16 cm test section), for 0.27 mm, 0.8 mm and 1.1 mm silica sand particles; ----- calculated, _____ measured (reproduced from Colakyan (9)).

V. EXPERIMENTAL RESULTS

A. Calculation of Heat Transfer Coefficients

The mean heat transfer coefficient h is calculated for each run using the following relationship. The values of the coefficients are shown in Tables (A.1, A.2, A.3)-Appendix.

$$h = \frac{P}{A_T (T_R - T_S)} \quad (V.1)$$

where A_T = surface area of the finned tube available for heat transfer (0.09243 m²)

P = power input to the heater (W)

T_S = bulk temperature of the solids (K)

T_R = steady-state average surface temperature of the rod (K)

Operating temperatures of the measuring element were selected based on the following criteria.

First, the rod should not exceed 100^oC, to avoid possible damage to the epoxy adhesive used to hold the thermocouples in place.

Second, considering the type of material used in the experiment. For example, in case of polyethylene temperature of the rod should not exceed 90^oC. In preliminary runs of the experiment this material was melted at higher temperatures regardless of the velocity of the moving particles.

Third, minimization of computational errors was achieved by providing the maximum possible temperature difference $T_R - T_S$. The arithmetic mean of temperature differences between the transfer surface and the moving bed was used because of the small variation in the temperature difference across the length of the tube.

The power dissipation to the moving bed was calculated from the equation

$$P = \frac{V^2}{R_{\Omega}} \quad (V.2)$$

where V was the measured voltage across the heater and R was the resistance of the cartridge heater, experimentally found to be 11.287Ω . This value was taken as the average of the resistances at a temperature of about 80°C . All the measured resistances at different temperatures showed a maximum variation of ± 2 percent from the above value.

B. Heat Transfer Results

The following section gives a graphical representation of the experimental results for overall heat transfer coefficient from an immersed finned tube and moving beds of solids. Comparison between the graphical presentations and the proposed model of Colakyan (9) are given in the subsequent pages.

Graphical Presentation

In the recent study by Colakyan (9) concerning plain tube, it was observed that heat transfer coefficient for the same material, i.e., polyethylene is higher for the smaller particle size. Also, the rate of increase of heat transfer coefficient is greater at lower velocities of solids. Figure (V.1) presents the value of heat transfer coefficients as a function of the linear velocity of the solids for polyethylene particles of 0.85 mm and 1.6 mm diameter. In the present study with the finned cylinder the same results as for the plain tube were obtained as shown in Figures (V.2 and V.3).

As determined earlier by Harakas and Beatty (2), Botterill (10) and Colakyan (9), materials with higher thermal diffusivity gave higher heat transfer coefficients. As an example, the data for polyethylene $d_p = 0.85$ mm, and silica sand $d_p = 0.8$ mm, as well as for copper $d_p = 0.85$ and silica sand $d_p = 0.8$ mm are presented collectively in Figures (V.4 and V.5).

Due to the nature of work involving similar material for different experiments, not all the graphs of the experiments are included in this chapter, but the results of individual experiments are given in Tables (A.1, A.2, A.3)-Appendix.

On the basis of experimental results an attempt has been made to explain the results and develop a correlational equation for heat transfer to flowing solids for extended immersed surfaces. These are discussed in detail in the following chapter.

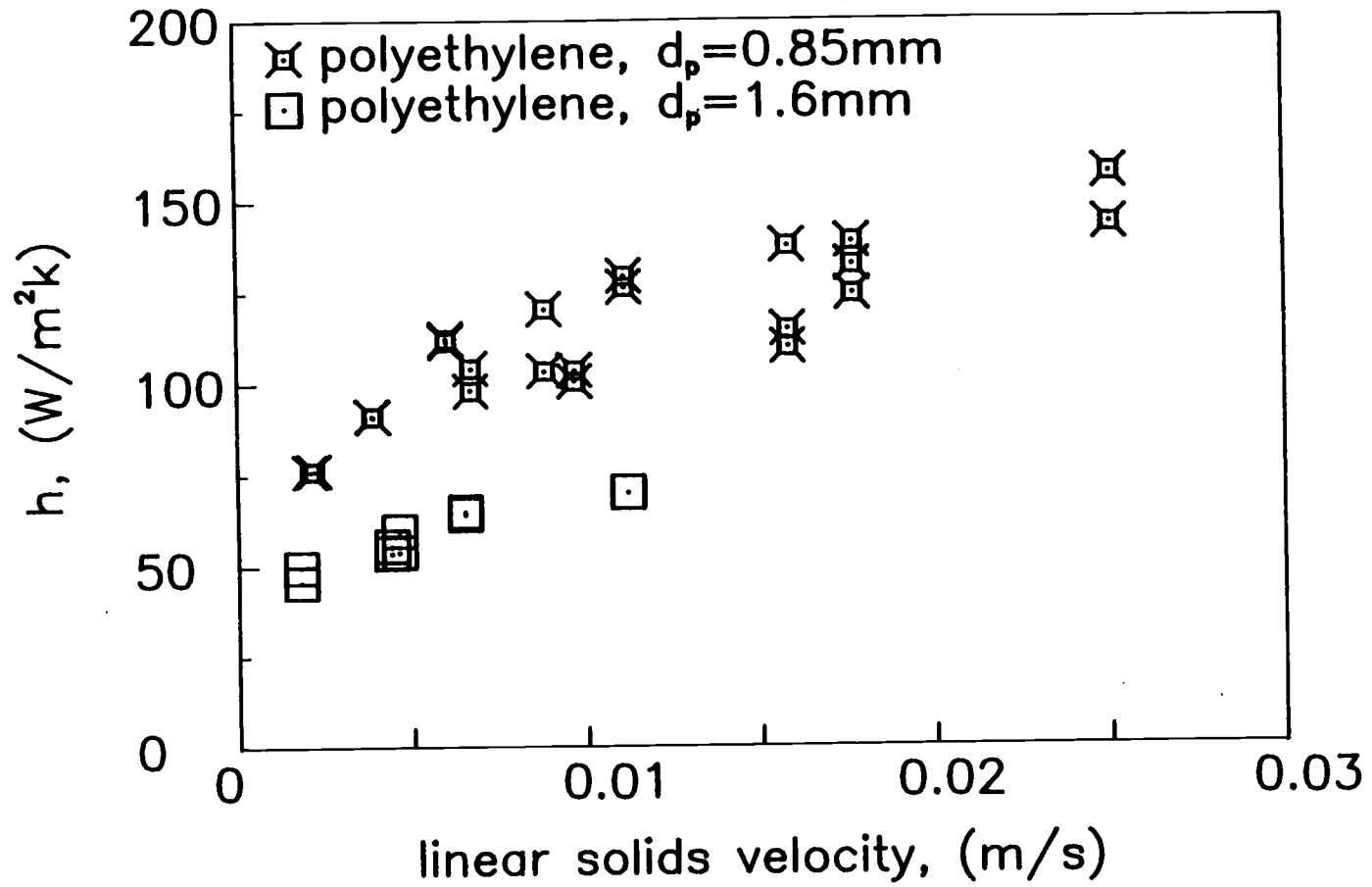


Figure (V.1). Comparison between heat transfer coefficients as a function of the linear velocity of the solids for polyethylene particles of 0.85 mm and 1.6 mm in diameter.

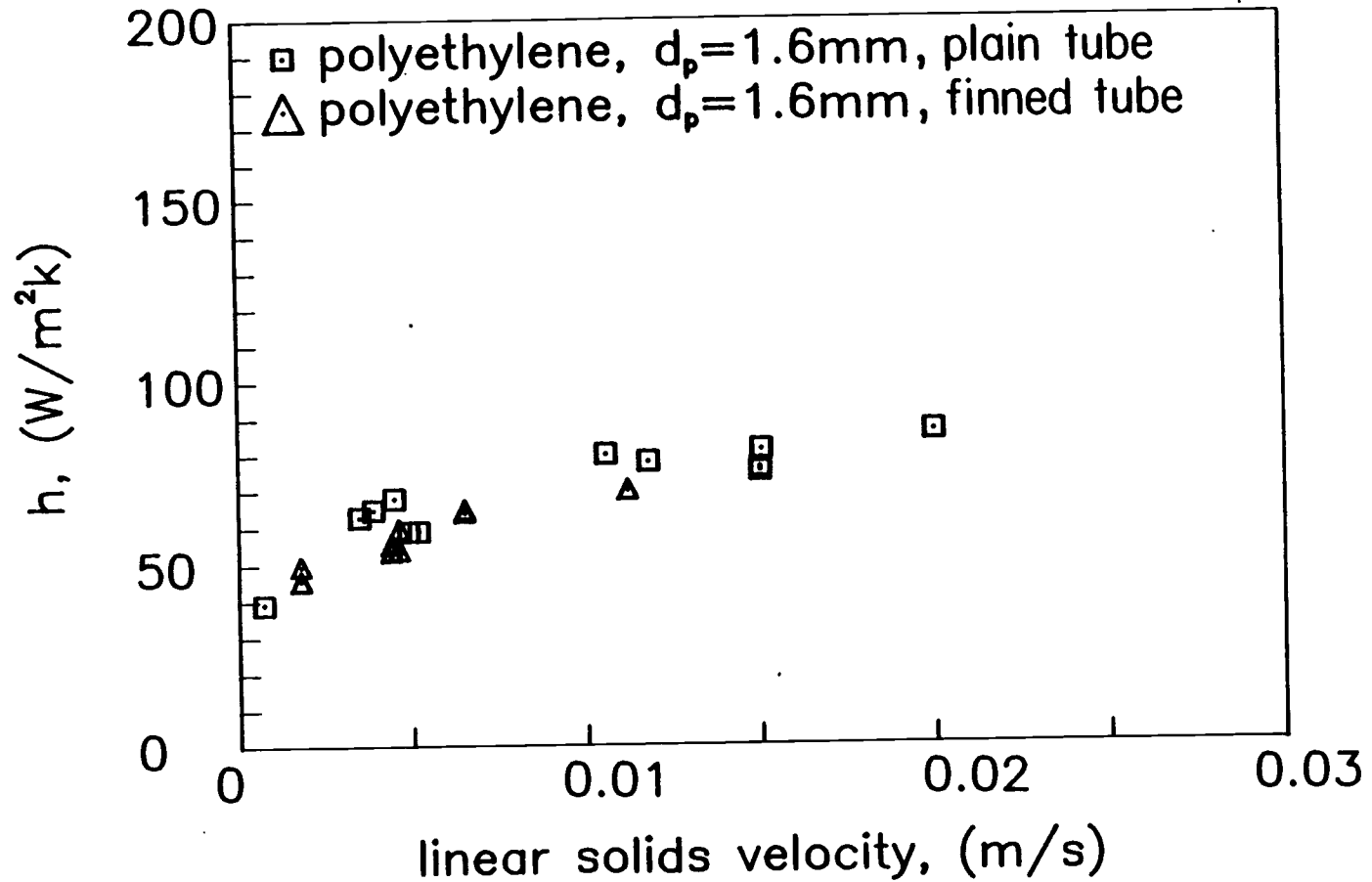


Figure (V.2). Comparison between the heat transfer coefficients for a finned and plain tube for polyethylene particles of 1.6 mm in diameter.

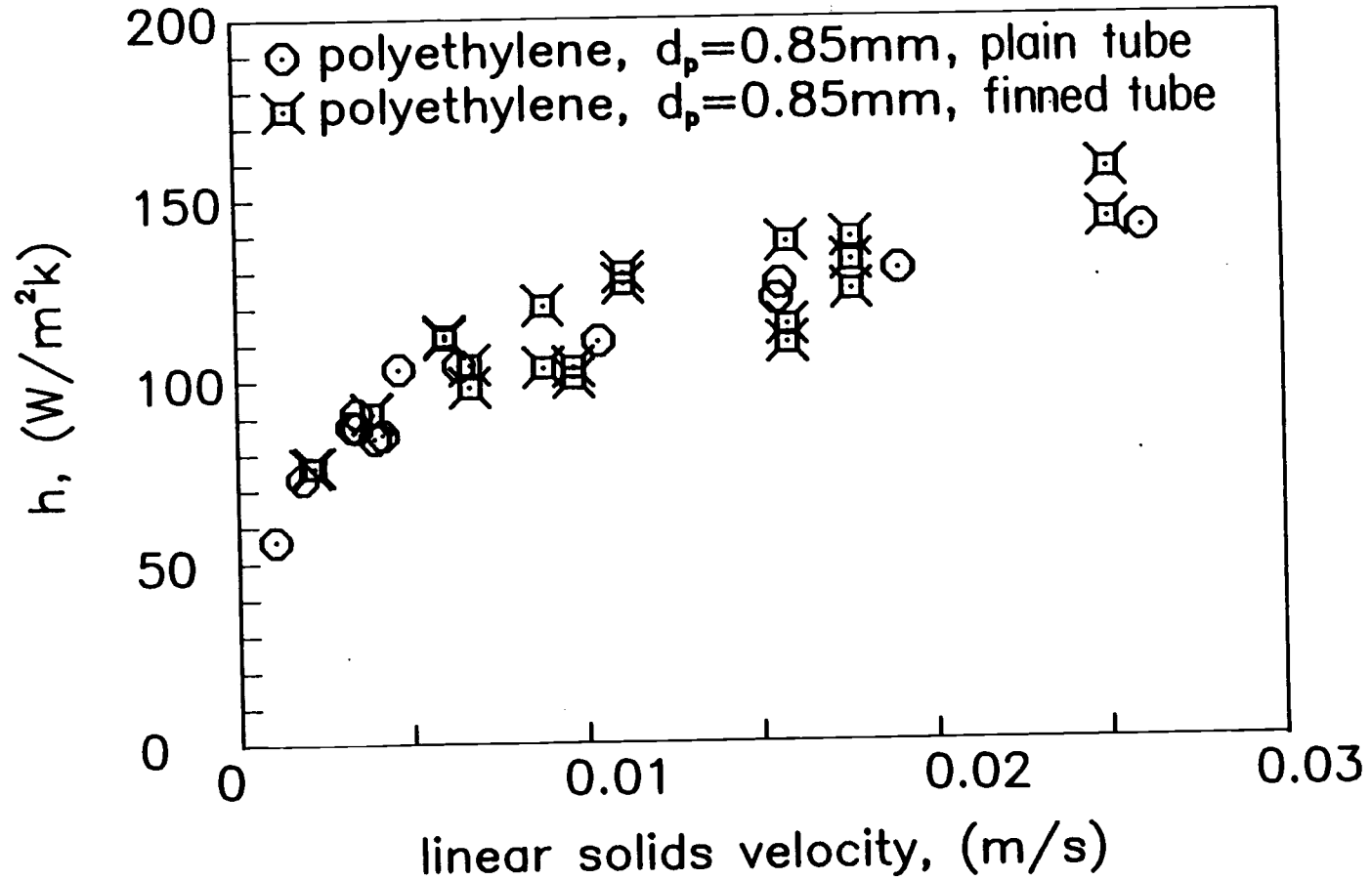


Figure (V.3). Comparison between the heat transfer coefficients for a finned and plain tube for polyethylene particles of 0.85 mm in diameter.

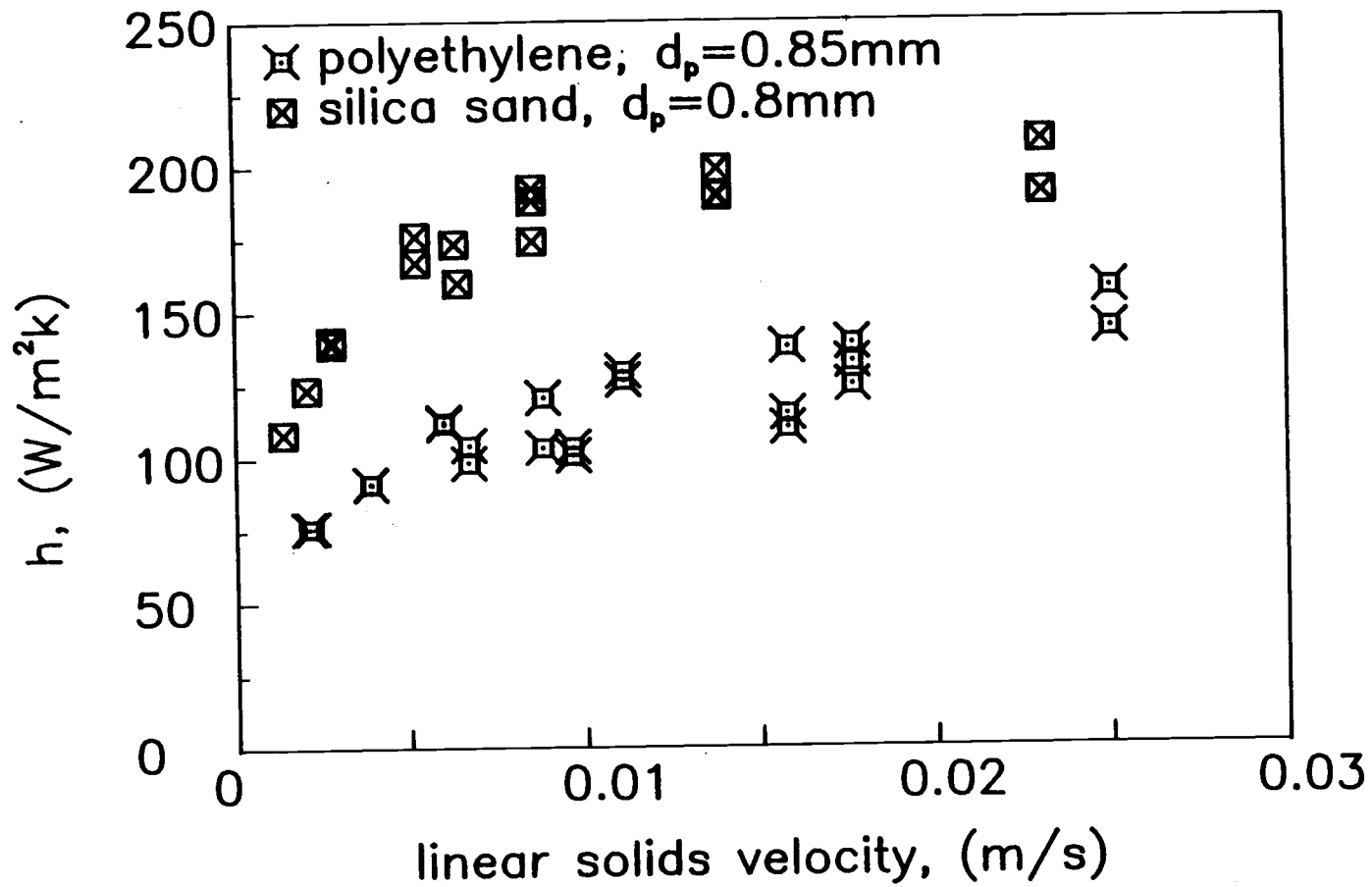


Figure (V.4). Comparison between heat transfer coefficients for polyethylene and silica sand with diameters 0.85 mm and 0.8 mm, respectively.

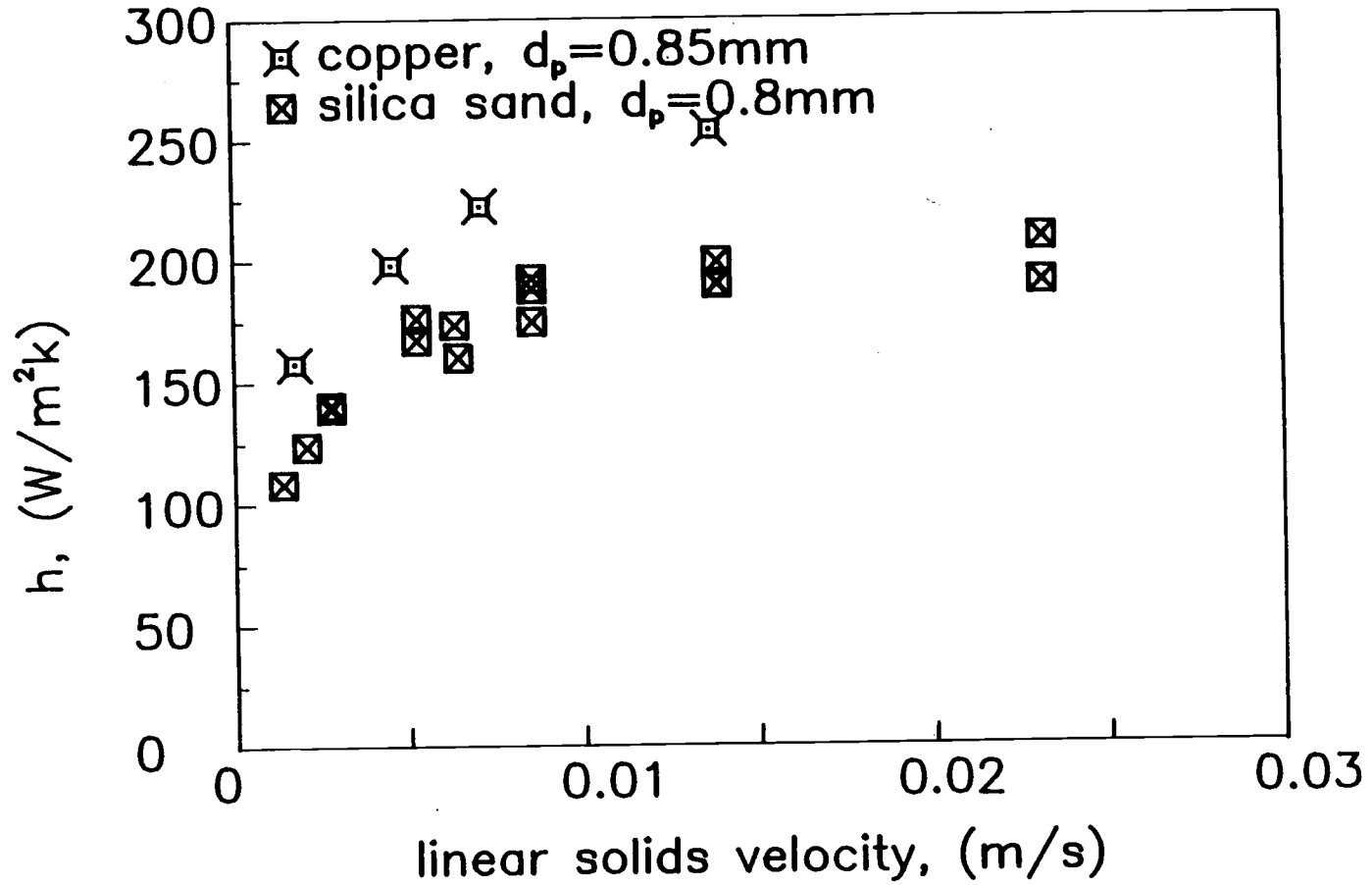


Figure (V.5). Comparison between heat transfer coefficients for copper and silica sand with diameters 0.85 mm and 0.8 mm, respectively.

VI. CORRELATION EQUATION

The complicated geometrical shape of transverse finned tube makes an analytical study of the system very difficult. In the following analysis a general correlation equation is developed which is applicable for a wide range of particle sizes and thermal diffusivities. It is assumed that the moving packed bed consists of a granular media and the interstitial fluid (air) moving passively with the solids at uniform velocity. Such a system is considered as a one-component entity (modification of the "packet" theory). This is a reasonable assumption for low solid velocities and fine particles (Colaykan (9)).

To determine a set of dimensionless groups, with which experimental data for heat transfer coefficient between solids and the heated surface be correlated, Buckingham's Pi method was applied (Perry (11)). Variables taken into account because of their assumed influence on the heat transfer coefficient are given below.

- d_p = particle diameter
- ρ_b = bulk density
- C_{ps} = heat capacity of solids
- k_e = effective thermal conductivity of the gas-solids system
- k_g = thermal gas conductivity
- U_s = solids velocity

Three dimensionless groups result from the dimensional analysis:

$$P_e = \frac{C_{ps} d_p \rho_b U_s}{k_g} \quad \text{Peclet Number (VI.1)}$$

where $Nu_d = \frac{h d_p}{k_g} =$ Nusselt number (VI.2)

$\frac{k_e}{k_g}$ - ratio of the effective and gas thermal conductivities

$\frac{d_p}{L}$ - ratio of particle diameter to the length of heater across the flow path of solids

where L is calculated from the following formula:

$$L = L_B \cdot \frac{A_B}{A_T} + L_F \left(1 - \frac{A_B}{A_T}\right) \quad \text{(VI.3)}$$

$$L_B = r \cdot \pi \quad \text{(VI.4)}$$

$$L_F = \frac{(R + r) \pi}{2} \quad \text{(VI.5)}$$

$$A_B = r \cdot \pi (L_R - N_F \cdot \delta_F) \quad \text{(VI.6)}$$

$$N_F = 54 \quad \text{(number of fins)}$$

$$\delta_F = \text{fin thickness (m)}$$

$$L_R = \text{length of the finned tube (m)}$$

The correlation developed was of the form

$$Nu_d = b_1 (Pe)^{b_2} \left(\frac{k_e}{k_g}\right)^{b_3} \left(\frac{d}{L}\right)^{b_4} \quad (VI.7)$$

The values of the constraints b_1 , b_2 , b_3 , b_4 were estimated by applying nonlinear regression analysis. They were determined to be 2.37, 0.25, 0.30, 0.33, respectively. Thus

$$Nu_d = 2.37 Pe^{0.25} \left(\frac{k_e}{k_g}\right)^{0.30} \left(\frac{d}{L}\right)^{0.33} \quad (VI.8)$$

The comparison between the observed and predicted values of Nu_d are displayed in Figure (VI.1).

The results calculated by applying the correlation equation to Colakyan's (9) data alone and to Colakyan's (9) and the author's data are shown in Figure (VI.2 and VI.3), respectively. It is evident from the graph that the heat transfer coefficient can be adequately predicted for the plain tube as well as for a tube with extended surfaces by the Equation (VI.8). Most of the values lie within a ± 20 percent deviation of the value predicted by the equation. Since only one fin type was examined some deviations from the proposed Equation (VI.8) can be expected for other types or other sizes of finned tubes. For very large fin spacing the shape approaches a horizontal tube, so good agreement with the Equation (VI.8) would be expected. For various fin heights some deviation from Equation (VI.8) might be expected. However, Equation (VI.8) can probably be applied to all fin heights equal to or less than that used in this work.

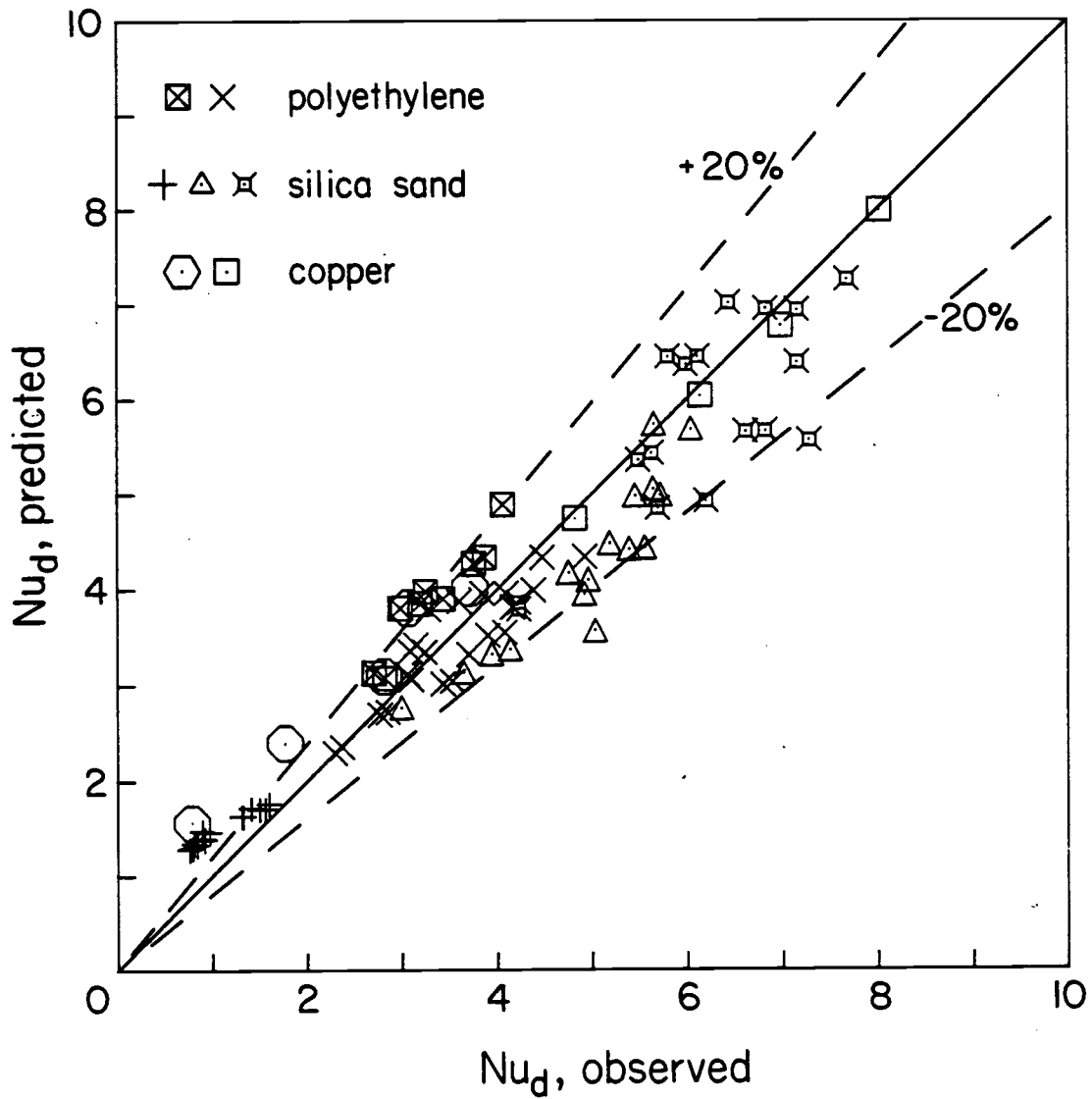


Figure (VI.1). Predicted (from Equation VI.8) and observed Nusselt numbers for all particles and sizes used for the experiments.

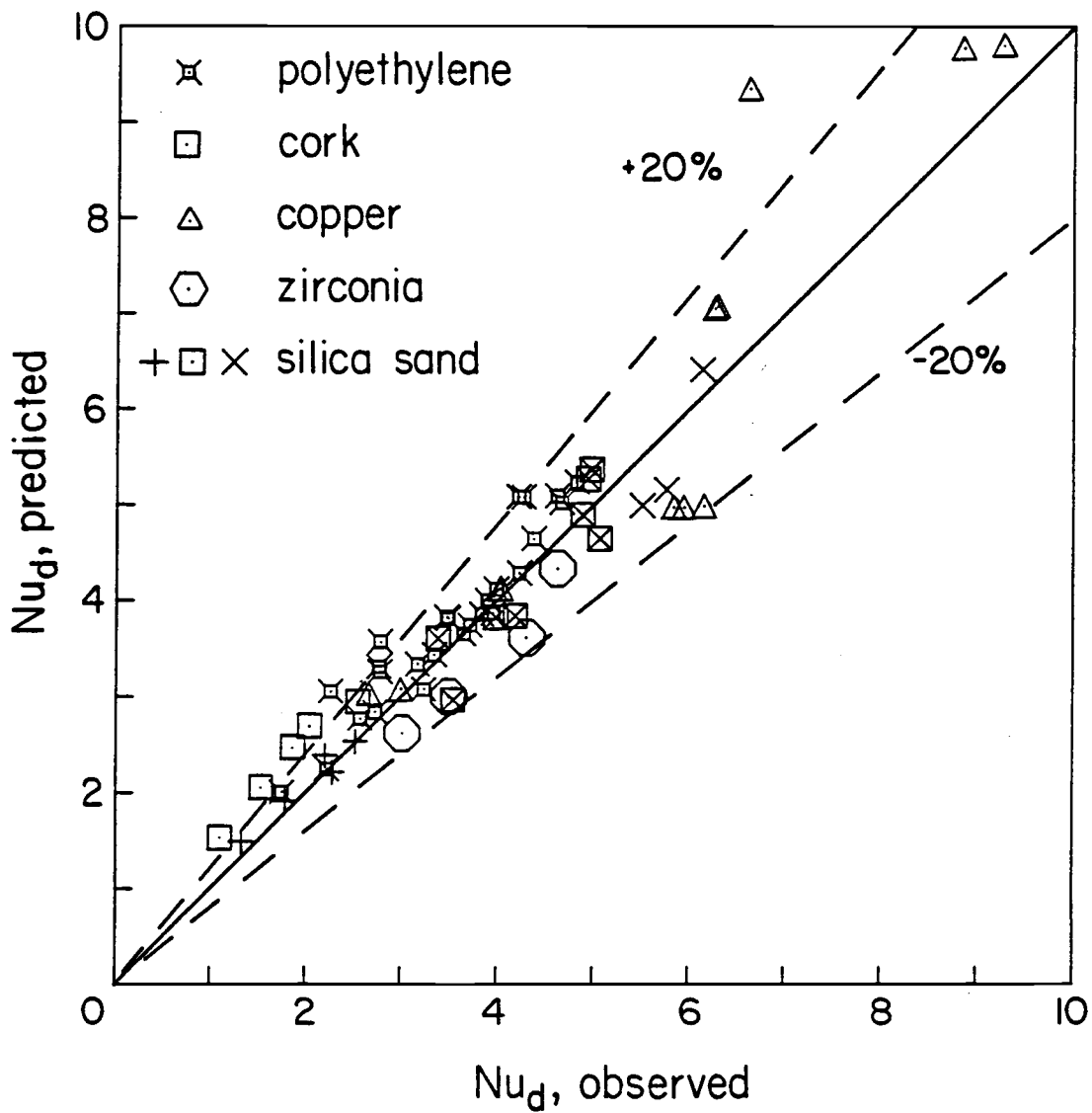


Figure (VI.2). Predicted (from Equation VI.8) and observed Nusselt numbers for all particles and sizes (data for heat transfer coefficients taken from Colakyan (9)).

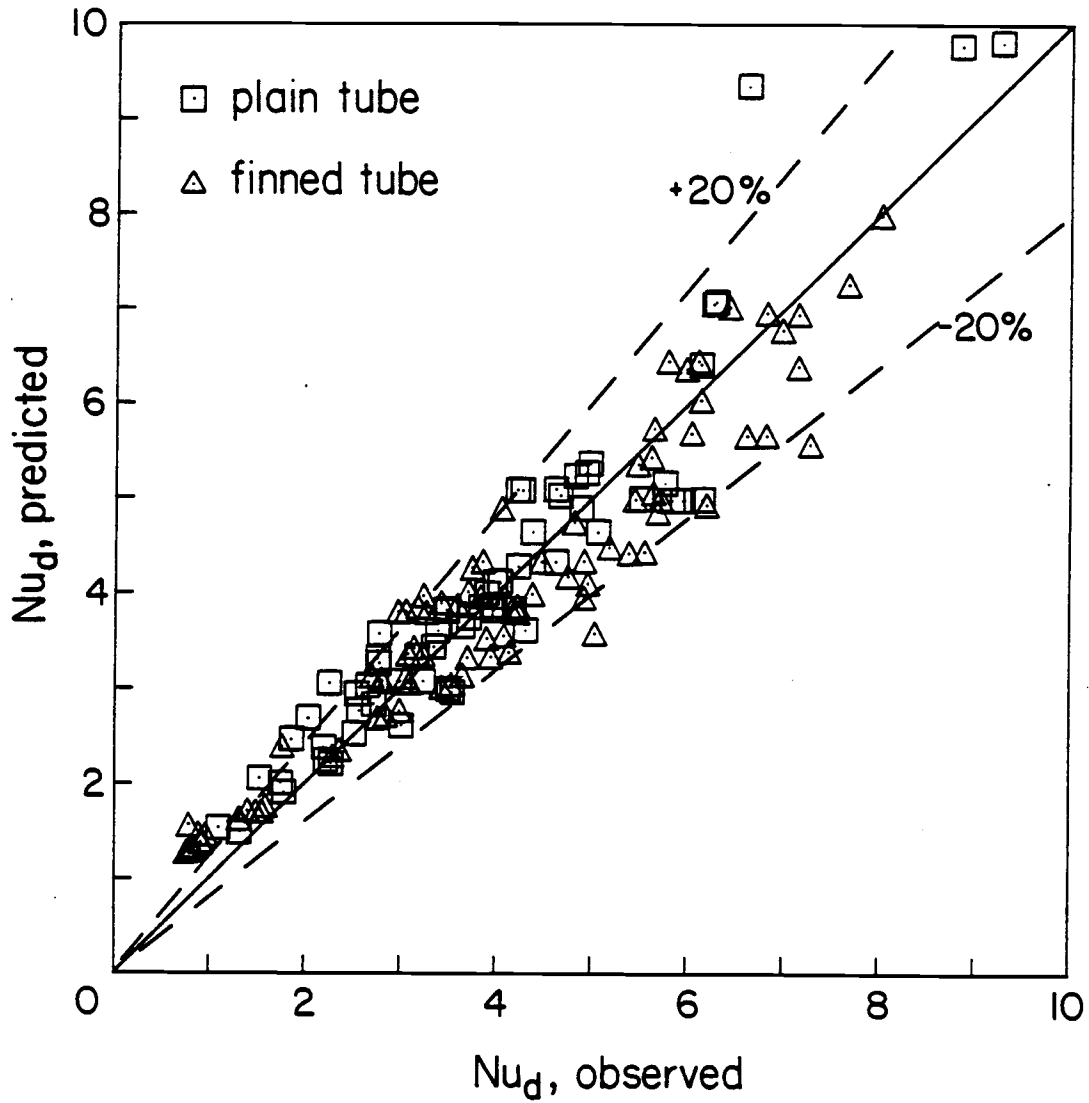


Figure (VI.3). Predicted (from Equation VI.8) and observed Nusselt numbers for Colakyan's (9) and author's data for all particles and sizes.

VII. DISCUSSION OF COLAKYAN'S MODEL

A. Colakyan's Work

Colakyan (9) in his Ph.D. thesis presented a model for heat transfer from a heated surface to flowing solids. Since this research involves the same principle considerable reference is made to his work. He based his research on the assumption that the solids flowing over a heated surface and the interstitial gas act as a one component entity flowing over the heated surface with a uniform velocity. (This assumption is a modification of the packet theory.)

In his work he shows that the unsteady state heat transfer to the semi-infinite plane above a heated tube or plate is almost the same, i.e., both conditions overpredict the heat transfer coefficients after $U_s = 0.005$ m/s, as shown in Figure (VII.1) (Colakyan (9)). Because of its simplicity, he used the flat plate solution for calculations involving the heat transfer coefficient. Therefore he described the unsteady-state heat transfer to the semi-infinite plane above the plate by the equation

$$\frac{\partial T}{\partial t} = \frac{k_e}{\rho_b C_{ps}} \frac{\partial^2 T}{\partial y^2} \quad (\text{VII.1})$$

by substituting the time t , by $t = \frac{x}{U_s}$ in the above equation the following results

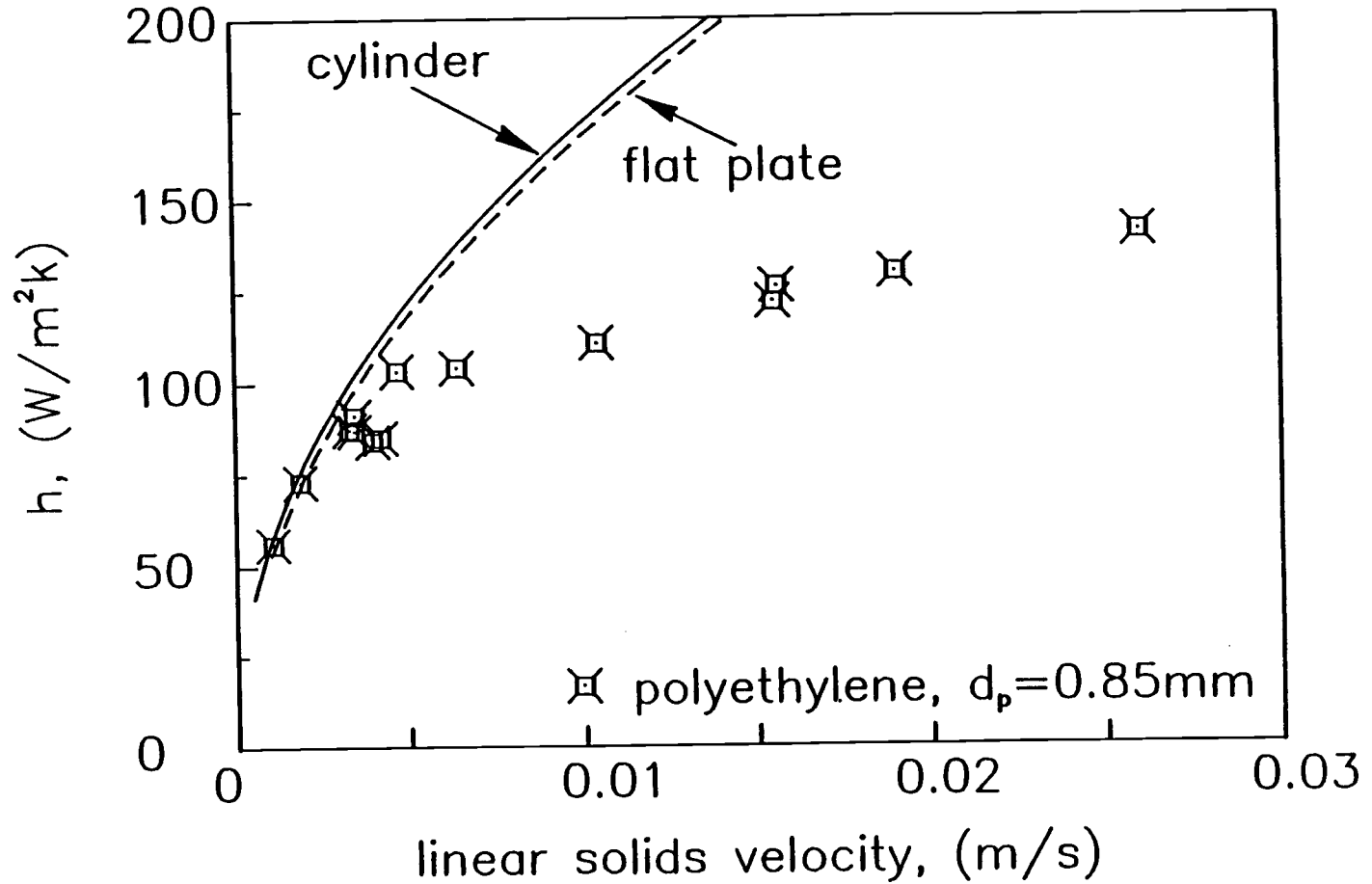


Figure (VII.1). Comparison of the continuum model for planar and cylindrical geometries with a set of experimental data (reproduced from Colakyan (9)).

$$U_s \frac{\partial T}{\partial x} = \frac{k_e}{\rho_b C_{ps}} \frac{\partial^2 T}{\partial y^2} \quad (\text{VII.2})$$

with the following initial and boundary conditions

$$\begin{aligned} x = 0 & \quad T = T_s \quad (\text{solids bulk temperature}) \\ y = 0 & \quad T = T_w \quad (\text{constant heater surface temperature}) \\ y \rightarrow \infty & \quad T = T_s \end{aligned}$$

where

x = coordinate in the direction of flow

y = coordinate in the direction perpendicular to the plate

U_s = solids velocity

k_e = effective thermal conductivity of the solids-gas entity or solids emulsion

ρ_b = bulk density of the solids-gas entity

C_{ps} = heat capacity of the solids gas entity, approximately equal to the heat capacity of solids alone

T = temperature, $T(x,y)$ of solids-gas entity at the " x " and " y " position

Carslaw and Jaeger (12) expressed the instantaneous coefficient (h_i) by the equation

$$h_i = \sqrt{\frac{C_{ps} k_e \rho_b U_s}{\pi X}} \quad (\text{VII.3})$$

and if the heater length across the flow path of the solids is L , then the average heat transfer coefficient is given by

$$\begin{aligned} h &= \frac{\int_0^L h_i dx}{L} = 2 \sqrt{\frac{C_{ps} k_e \rho_b U_s}{\pi L}} \\ &= 2 \sqrt{\frac{C_{ps} k_e \rho_b}{\pi t}} \quad (\text{VII.3a}) \end{aligned}$$

where t represents the contact time of the solids emulsion with the heater surface.

Yagi and Kunii (13) experimentally estimated the effective thermal conductivities of packed beds, without an imposed pressure drop across the bed. It was observed that the gas travelled at the same velocity as the solids, and thus was assumed to be motionless with respect to the solids. The effective thermal conductivity is expressed by the following relationship

$$\frac{k_e}{k_g} \approx \frac{1 - \epsilon}{\frac{k_g}{k_s} + \psi} \quad (\text{VII.4})$$

where ϵ is the fraction of the voids and ψ was taken to be approximately

$$\psi = 0.2 \epsilon^2 \quad (\text{VII.5})$$

and the bulk density of the flowing solids is estimated by the following equation

$$\rho_b = \frac{W_s}{U_s A} \quad (\text{VII.6})$$

where A is the area of flow and W_s is the mass flow rate. It was observed during the experiments that the bulk density of the flowing solids was almost equal to the bulk density of the packed bed.

Colakyan in his work concluded that for fine particles or very low solids velocities (large contact interval) the assumption of the homogeneity of the flowing material are valid, but for large particles or very high solid velocity this assumption may not hold true as indicated in Figure VII.2 reproduced from Colaykan (9).

In the discussion to this point a single resistance to heat flow from the solid surface to the emulsion (and vice versa) has been considered as expressed by the equation

$$R_e = 0.5 \sqrt{\frac{\pi L}{C_{ps} k_e \rho_b U_s}} \quad (\text{VII.7})$$

$$1/R_e = 2 \sqrt{\frac{C_{ps} k_e \rho_b U_s}{\pi L}} \quad (\text{VII.7a})$$

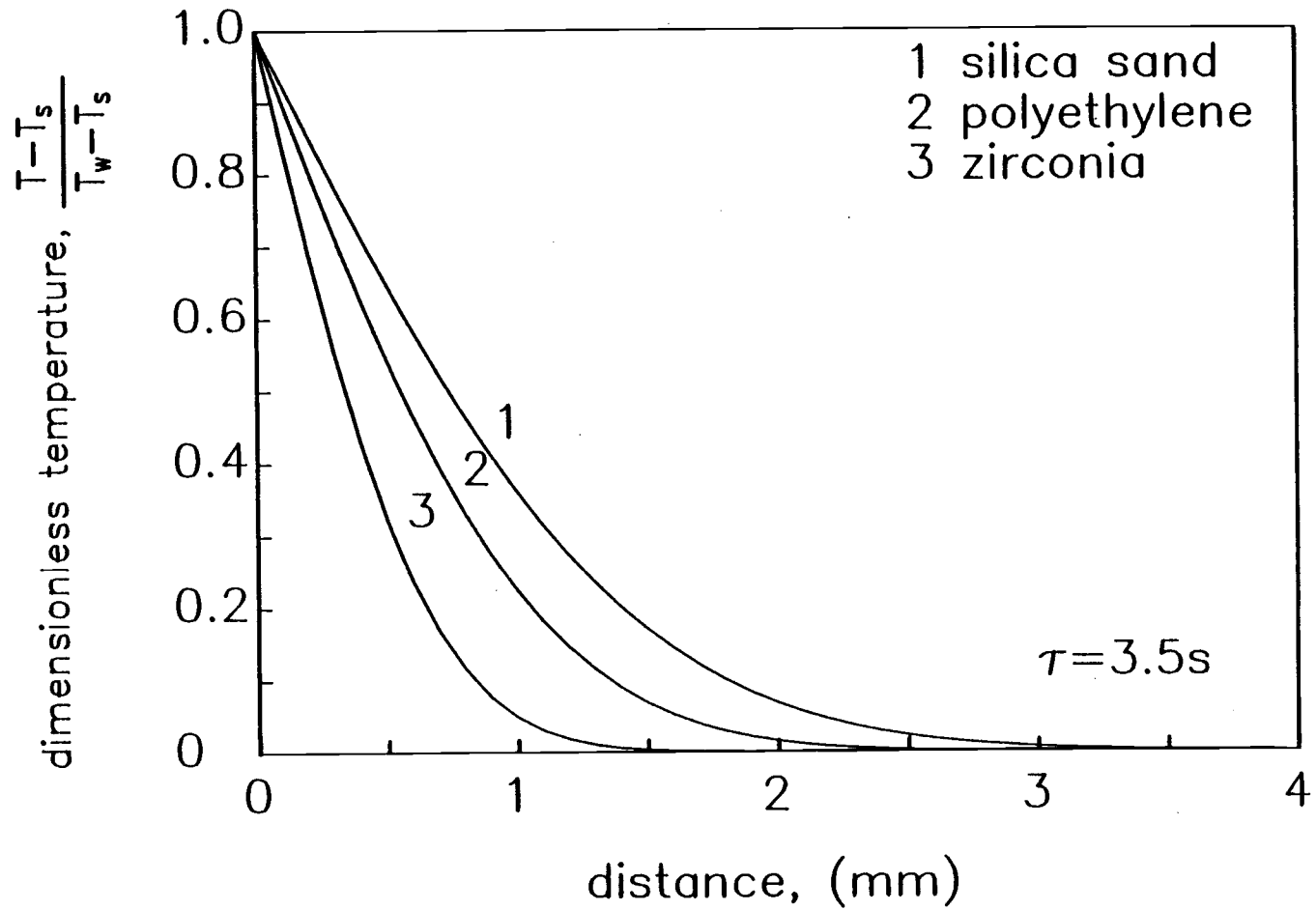


Figure (VII.2). Temperature profiles, in the semi-infinite plane above a constant temperature, heated flat plate, for a contact time of 3.5 s (reproduced from Colakyan (9)).

However, two resistances in series can also be considered:

1. a contact resistance, R_c , dependent upon increased voidage near the heat transfer surface and,
2. the resistance due to emulsion. Thus the overall average convective heat transfer coefficient may be expressed by the relation

$$h = \frac{1}{R_c + R_e} \quad (\text{VII.8})$$

where R_c is the contact resistance and R_e is the emulsion resistance.

During heat transfer conduction from the heated surface to the flowing particles takes place through an intervening gas film of average thickness, δ . Thus R_c can be expressed as

$$R_c = \frac{\delta}{k_g} \quad (\text{VII.9})$$

During Colakyan's research, R_c was taken to be a function of the particle diameter and its value was determined experimentally and is expressed by the following equation

$$R_c = \frac{6.7 \times 10^{-5} d_p^2}{k_g} = \frac{\delta}{k_g} \quad (\text{VII.9a})$$

The local emulsion resistance (R_{ex}) which is the inverse of the instantaneous heat coefficient can be substituted for R_e and thus the instantaneous resistance can be represented by

$$h_i = \frac{1}{R_c + R_{ex}} \quad (\text{VII.8a})$$

By replacing h_i by \bar{h}_i the average heat transfer coefficient can be equated by the expression

$$h = \frac{\int_0^L \bar{h}_i dx}{L} = \frac{2}{R_{eL}} \left[1 - \frac{R_e}{R_{eL}} \ln \left(1 + \frac{R_e}{R_c} \right) \right] \quad (\text{VII.9})$$

where

$$R_{eL} = \sqrt{\frac{\pi L}{\rho_e k_e C_{ps} U_s}} \quad \text{OR} \quad \sqrt{\frac{\pi t}{\rho_e k_e C_{ps}}} \quad (\text{VII.10})$$

Simplifying the above equations for heat transfer coefficient the following equation results

$$h = \frac{1}{R_c + \frac{1}{L} \int_0^L h_i dx} = \frac{1}{R_c + 0.5 \sqrt{\frac{\pi t}{k_e \rho_b C_{ps}}}} \quad (\text{VII.11})$$

Colakyan (9) fitted this equation to his data and obtained good agreement (Figure VII.3 and VII.4). (For more details refer to Colakyan (9).)

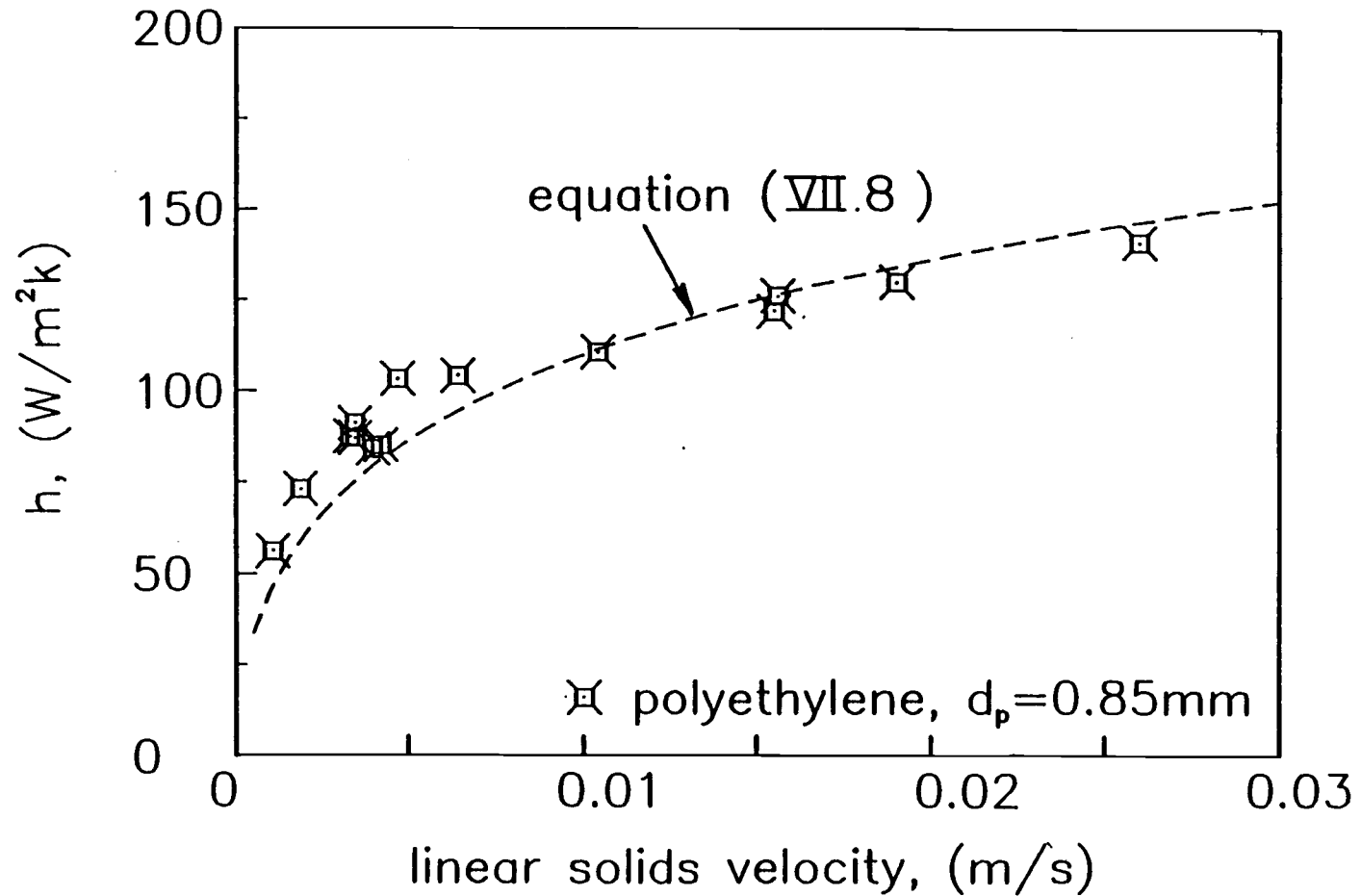


Figure (VII.3). A comparison of model predictions (two thermal resistances, R_e and R_c , in series with $R_c = 0.00168 \text{ m}^2\text{K/W}$) with experimental results, for 0.85 mm polyethylene particles (reproduced from Colakyan (9)).

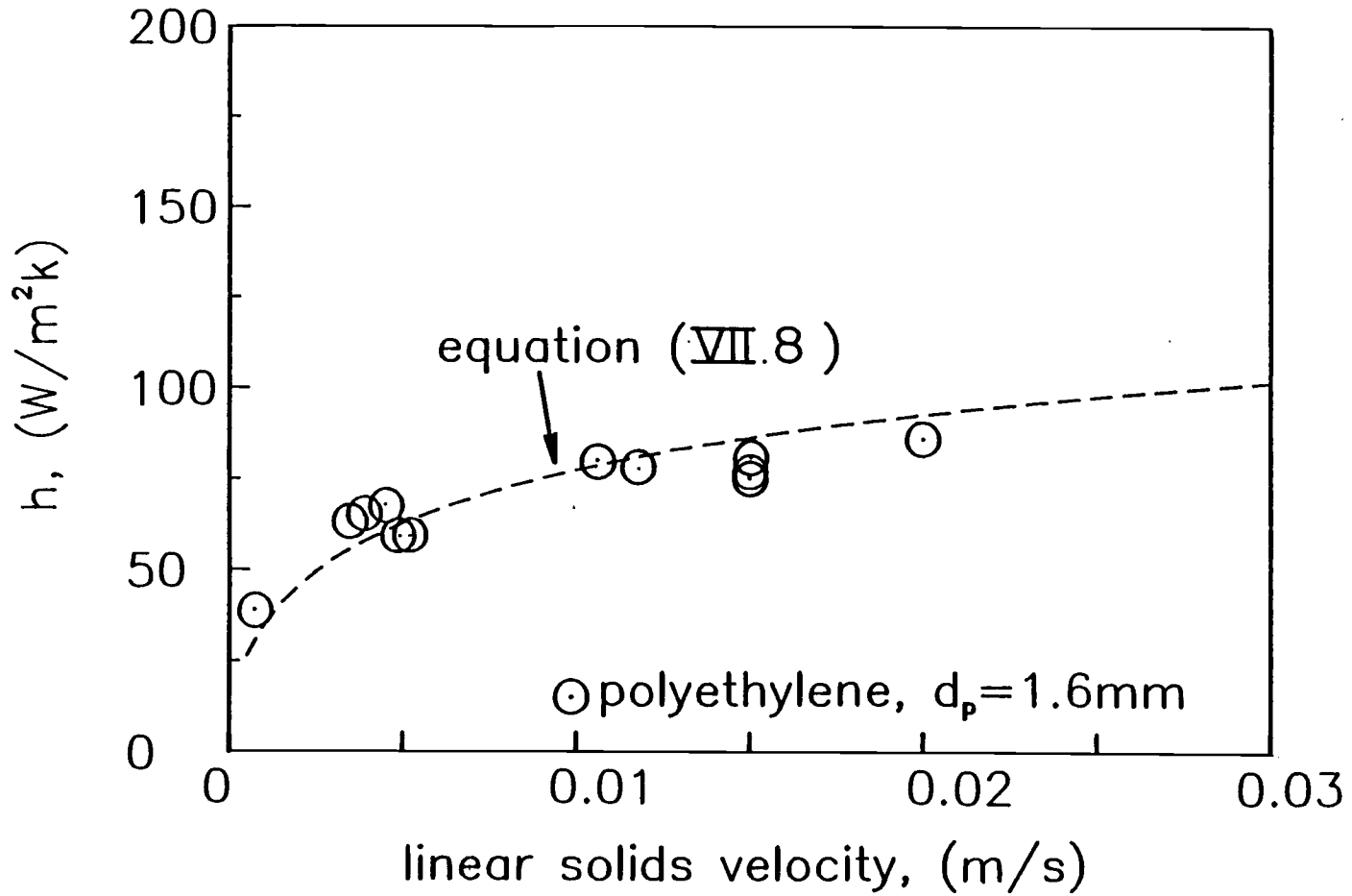


Figure (VII.4). A comparison of model predictions (two thermal resistances, R_e and R_c , in series with $R_c = 0.0057 \text{ m}^2\text{K/W}$) with experimental results, for 1.6mm polyethylene particles (reproduced from Colakyan (9)).

The average conduction thickness was approximately 10 percent of the particle diameter of the large particles (i.e., 1mm and above) and its value decreased with decreasing particle diameter.

The overall heat transfer coefficient, i.e.,

$$h = \frac{1}{R_c + R_e} \quad (\text{VII.8})$$

can be expressed in the following manner by replacing R_c and R_e with their equivalent expressions

$$h = \frac{1}{\frac{6.7 \times 10^{-5} d_p^2}{k_g} + 0.5 \sqrt{\frac{\pi t}{k_e \rho_b C_{ps}}}} \quad (\text{VII.12})$$

This equation predicted about 85 percent of the observed values within ± 20 percent deviation as shown in Figure (VII.5) (reproduced from Colakyan (9)).

B. Analysis of Colakyan's Model

In his work Colakyan made several assumptions which were investigated during the present work. Two of them do not appear to be to the present results. These two assumptions are:

1. The overall resistance to the heat transfer between heated surface and the granular material is the sum of the resistances R_c and R_e which are in series, Baskakov (4) where

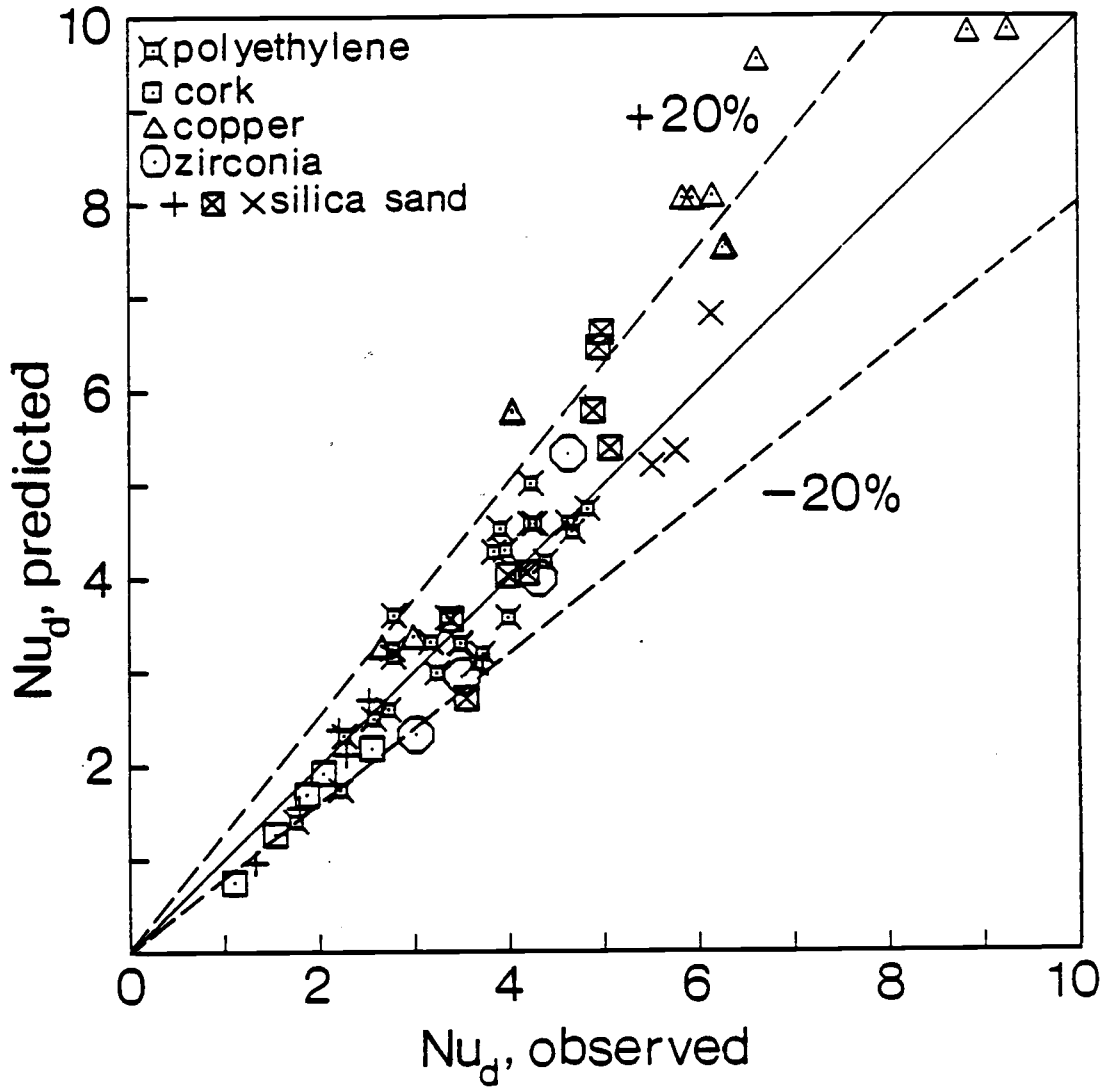


Figure (VII.5). Predicted (from Equation VII.12) and observed Nusselt numbers, for all particles and sizes (reproduced from Colakyan (9)).

R_c = contact resistance

R_e = emulsion resistance

2. Contact resistance (R_c) is time independent, i.e., conduction through the gas boundary layer.

It appears that the assumption for the resistances in series seems acceptable in fluidized beds, but not for moving beds, i.e., constant contact between particles and heated surface and larger contact area.

To support this inference R_c was recalculated from the formula

$$h = \frac{1}{R_c + R_e} \quad (\text{VII.8})$$

Thus,

$$R_c = \frac{1}{h} - R_e \quad (\text{VII.13})$$

where h is experimentally measured and R_e is estimated separately for each value of h under the same circumstances.

In case that the above stated assumption holds true, then R_c should be the function of velocity. This leads to the conclusion that if resistances are arranged in some other pattern (parallel) or more complex (series-parallel) one could expect negative values for contact resistance (R_c).

The graphical results obtained from Figure (VII.6) confirmed the author's expectations.

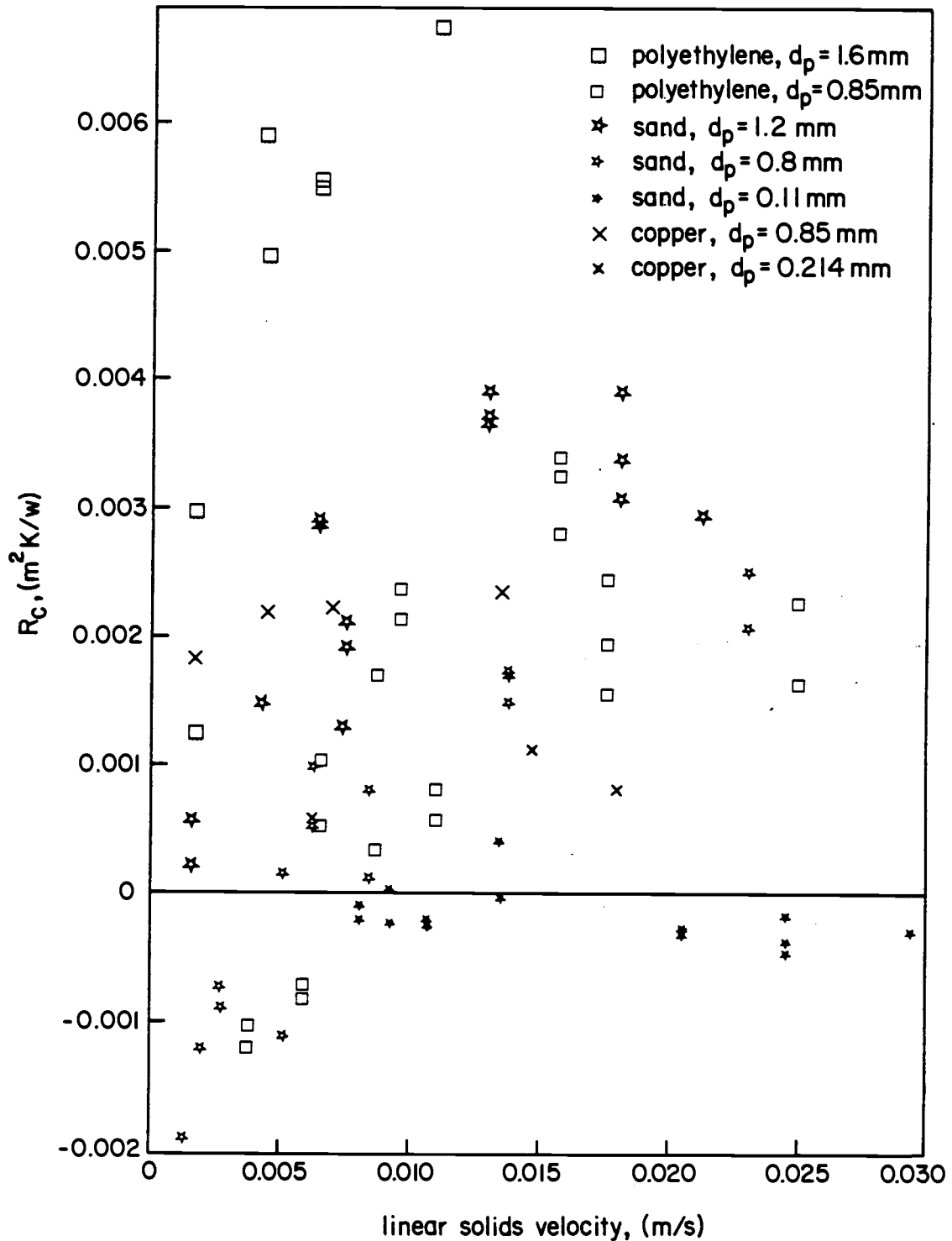


Figure (VII.6). Contact resistance (R_c) vs. linear solids velocities for all particles and sizes.

Unfortunately, these findings are not enough to fully understand the mechanism involved in the heat transfer between the heated surface and moving beds of particles.

The trend of R_c depicted from the equation (VII.13) can be the result of the fact that resistances R_c and R_e are in parallel or in series-parallel arrangement. It can also be due to the fact that the formula for R_e is not correct.

The theory of resistances in series first proposed by Baskakov (4) may hold true for all the particles in the moving beds except for the very first layer of the particles that are adjacent to the heating surface. At this location there might exist a more complex relationship between the resistances.

The author believes that these conclusions can be the basis for future research.

It is important to point out here, that the main scope of the present research was to find a correlational equation which can be applied to industrial problems (Equation VI.8).

Fundamental knowledge pertaining to the mechanism of heat transfer between immersed surfaces and moving beds of granular media requires further experimental and theoretical study.

VIII. CONCLUDING STATEMENTS

The heat transfer coefficient between a single finned tube and moving beds of solids was measured under atmospheric pressure, in which the interstitial fluid (air) is carried along with the solids. Such a system is considered as a one component entity (derived from the packet theory).

An empirical equation was developed employing dimensional analysis and non-linear regression of the experimental data.

$$Nu_d = 2.37 Pe_d^{0.25} \left(\frac{k_e}{k_g}\right)^{0.3} \left(\frac{d}{L}\right)^{0.33} \quad (VI.8)$$

This equation predicts the heat transfer coefficients for plain and finned tubes within ± 20 percent.

Since only one type of finned tube was used the applicability should be restricted to the tubes with fin heights equal to or smaller than that used for this research.

The model of heat transfer with two resistances in series is expressed by the following equation

$$h = \frac{1}{R_c + R_e} \quad (VII.8)$$

where

1. R_e is the resistance generated due to the solid-gas emulsion, surrounding the heat transfer surface (adapted

from the "packet" theory of heat transfer in fluidized beds).

2. R_c is the contact resistance (conduction through the gas boundary layer) and is time independent.

The above equation was not applied to the present research, because of the author's doubts as to the validity of such model for moving granular beds. From the experimental data R_c appeared to be dependent on time (Figure (VII.6)). This leads to the conclusion that resistances (R_e and R_c) could be in parallel or even more complex arrangements (series-parallel). The deviation from the Equation (VII.13) can also be due to the fact that it does not fully explain the role of R_e , in the system and that R_e , can influence the system in a way which is not as yet well understood.

BIBLIOGRAPHY

BIBLIOGRAPHY

1. Mickly, H.S. and D.F. Fairbanks, "Mechanisms of Heat Transfer to Fluidized Beds, AICHe J., 1 374 (1955).
2. Harakas, N.K. and K.O. Beatty, Jr., "Moving Bed Heat Transfer: Effect of Interstitial Gas with Fine Particles," Chem. Eng. Prog. Symp. Ser., 59, No. 41, pp. 122-128 (1963).
3. Sullivan, W.N. and R.H. Sabersky, "Heat Transfer to Flowing Granular Media," Int. J. Heat and Mass Transfer, 18, 97 (1975).
4. Baskakov, A.P., "the Mechanism of Heat Transfer Between a Fluidized Bed and a Surface," Int. Chem. Eng., 4 320 (1964).
5. Denloye, A.O.O. and J.S.M. Botterill, "Heat Transfer in Flowing Packed Beds," Chem. Eng. Sci., 32, 461 (1977).
6. Spelt, Jan Karel, An Experimental Study of Heat Transfer to Flowing Granular Media, M.S. Thesis, California Institute of Technology, Pasadena, CA (1981).
7. Donskov, S.V., Teploenergetika, In Russian, 11 (1958).
8. Kurochkin, Yu P., Inzhenerno-Fizicheskifi Zhurnal, In Russian, 4, 76 (158).
9. Colakyan, Manuk, Moving Bed Heat Transfer and Fluidized Flutriation, Ph.D. Thesis, Oregon State University (1984).
10. Botterill, J.S.M., M.H.D. Butt, G.L. Cain and K.A. Redish, "The Effect of Gas and Solids Thermal Properties on the Rate of Heat Transfer to Gas-Fluidized Beds," International Symposium on Fluidization, Netherlands University Press, Amsterdam, p. 442 (1967).
11. Perry, R.H. and C.H. Chilton, Chemical Engineers' Handbook, 5th ed., McGraw-Hill Book Company, pp. 2-83 (1973).
12. Carslaw, H.S. and J.C. Jaeger, Conduction of Heat in Solids, Clarendon Press, Oxford, pp. 60-62 (1969).
13. Yagi, S. and D. Kunii, "Studies on Effective Thermal Conductivities in Packed Beds," AICHe J., 3, 373 (1957).
14. Eckert, E.R.G. and Robert M. Drake, Jr., Analysis of Heat and Mass Transfer, McGraw-Hill Book Company, p. 406 (1972).

15. Catipovic, N.M., Heat Transfer to Horizontal Tubes in Fluidized Beds: Experiment and Theory, Ph.D. Thesis, Oregon State University, pp. 110-127 (1979).
16. Kunii, D. and Octave Levenspiel, Fluidization Engineering, Robert E. Krieger Publishing Company, pp. 25, 195-219, 418-454 (1977).
17. McAdams, W.H., Heat Transmission, 3rd ed., McGraw-Hill, New York (1954).
18. Knudsen, J.G. and D.L. Katz, Fluid Dynamics and Heat Transfer, McGraw-Hill, New York (1958).
19. Welty, J.R., C.E. Wicks and R.E. Wilson, Fundamentals of Momentum, Heat, and Mass Transfer, 2nd ed., Wiley and Sons, New York (1976).

APPENDIX

APPENDIX A

Table A.1. Table of Experimental Conditions and Heat Transfer Coefficients for Polyethelene Particles.^{a/}

Run Number	Particle Diameter (m)	Linear Solids Velocity (m/s)	Mass Flow Rate (kg/s)	h_2 (W/m ² K)
1	0.0016	0.001807	0.0393	49.7
2	0.0016	0.001807	0.0393	45.4
3	0.0016	0.004415	0.0959	55.77
4	0.0016	0.004415	0.0959	53.694
5	0.0016	0.00463	0.1006	53.98
6	0.0016	0.00463	0.1006	59.82
7	0.0016	0.00653	0.14196	64.31
8	0.0016	0.00653	0.14196	64.91
9	0.0016	0.0112	0.2435	70.07
10	0.00085	0.0022	0.0507	76.23
11	0.00085	0.00209	0.0481	76.1
12	0.00085	0.00387	0.0892	91.2
13	0.00085	0.003896	0.0896	91.0
14	0.00085	0.006	0.13825	112.23
15	0.00085	0.006	0.13825	111.48
16	0.00085	0.0067	0.15438	98.02
17	0.00085	0.0067	0.15438	104.22
18	0.00085	0.008823	0.2033	103.35
19	0.00085	0.008823	0.2033	120.29
20	0.00085	0.009677	0.22297	100.43
21	0.00085	0.009677	0.22297	103.56
22	0.00085	0.01111	0.25576	129.3
23	0.00085	0.01111	0.25576	126.2
24	0.00085	0.0158	0.36405	114.55
25	0.00085	0.0158	0.36405	109.69
26	0.00085	0.0158	0.36405	137.52
27	0.00085	0.01765	0.40668	138.73
28	0.00085	0.01765	0.40668	132.275
29	0.00085	0.1765	0.40668	124.28
30	0.00085	0.025	0.57604	157.24
31	0.00085	0.025	0.57604	143.31

^{a/} $\rho_s = 920 \text{ kg/m}^3$; $k_s = 0.329 \text{ W/mK}$; $C_p = 2300 \text{ W}_s/\text{kgK}$

Table A.2. Table of Experimental Conditions and Heat Transfer Coefficients for Silica Sand Particles

Run Number	Particle Diameter (m)	Linear Solids Velocity (m/s)	Mass Flow Rate (kg/s)	h_2 (W/m ² K)
1	0.00011	0.00815	0.6572	194.0
2	0.00011	0.00815	0.6572	191.453
3	0.00011	0.0093	0.7499	197.86
4	0.00011	0.0093	0.7499	210.73
5	0.00011	0.01086	0.87575	225.08
6	0.00011	0.01086	0.87575	229.44
7	0.00011	0.01351	1.08945	218.56
8	0.00011	0.01351	1.08945	243.46
9	0.00011	0.02069	1.66844	328.46
10	0.00011	0.02069	1.66844	324.468
11	0.00011	0.02459	1.98293	340.828
12	0.00011	0.02459	1.98293	368.35
13	0.00011	0.02459	1.98293	380.863
14	0.00011	0.02933	2.36517	404.2
15	0.0008	0.00139	0.12193	108.19
16	0.0008	0.002069	0.18149	123.56
17	0.0008	0.00279	0.244737	140.29
18	0.0008	0.00279	0.244737	139.0
19	0.0008	0.00526	0.4614	167.07
20	0.0008	0.00526	0.4164	176.031
21	0.0008	0.006356	0.5575	173.29
22	0.0008	0.006451	0.56593	159.845
23	0.0008	0.00857	0.75175	174.37
24	0.0008	0.00857	0.75175	187.9
25	0.0008	0.00857	0.75175	192.146
26	0.0008	0.01385	1.2149	189.37
27	0.0008	0.01385	1.2149	190.0
28	0.0008	0.01385	1.2149	198.84
29	0.0008	0.0231	2.0263	190.285
30	0.0008	0.0231	2.0263	208.33
31	0.0012	0.001695	0.15377	102.27
32	0.0012	0.001695	0.15377	97.706
33	0.0012	0.004412	0.40026	141.394
34	0.0012	0.004412	0.40026	135.332
35	0.0012	0.006522	0.59167	129.87
36	0.0012	0.006522	0.59167	128.43
37	0.0012	0.0075	0.6804	170.5
38	0.0012	0.00769	0.6976	155.27
39	0.0012	0.00769	0.6976	150.928

Table A.2. continued

Run Number	Particle Diameter (m)	Linear Solids Velocity (m/s)	Mass Flow Rate (kg/s)	h_2 (W/m ² K)
40	0.0012	0.01304	1.18299	168.138
41	0.0012	0.01304	1.18299	142.06
42	0.0012	0.01304	1.18299	139.89
43	0.0012	0.01304	1.18299	132.9
44	0.0012	0.01818	1.6493	168.138
45	0.0012	0.01818	1.6493	146.98
46	0.0012	0.01818	1.6493	159.74
47	0.0012	0.02143	1.94413	178.596

a/ $\rho_s = 2700 \text{ kg/m}^3$; $k_s = 0.8 \text{ W/mK}$; $C_p = 780 \text{ W}_s/\text{kgK}$

Table A.3. Table of Experimental Conditions and Heat Transfer Coefficient for Copper Particles.^{a/}

Run Number	Particle Diameter (m)	Linear Solids Velocity (m/s)	Mass Flow Rate (kg/s)	h_2 (W/m ² K)
1	0.000214	0.00044	0.1486	103.85
2	0.000214	0.002365	0.799	223.54
3	0.000214	0.006416	2.1676	348.92
4	0.000214	0.0148	5.0	381.08
5	0.000214	0.0181	6.115	456.275
6	0.00085	0.00175	0.574	157.6
7	0.00085	0.00455	1.492	198.09
8	0.00085	0.00712	2.334	222.12
9	0.00085	0.01368	4.4852	253.6

^{a/} $\rho_s = 8954 \text{ kg/m}^3$; $k_s = 384 \text{ W/mK}$; $C_p = 383 \text{ W}_s/\text{kgK}$